Int J Coal Sci Technol (2017) 4(2):129–146
DOI 10.1007/s40789-017-0161-6

Effects of coal rank on physicochemical properties of coal and on methane adsorption

Yuanping Cheng[1,2] · Haina Jiang[3] · Xiaolei Zhang[4] · Jiaqing Cui[3] · Cheng Song[3] · Xuanliang Li[3]

Received: 25 September 2016 / Revised: 21 November 2016 / Accepted: 2 March 2017 / Published online: 27 March 2017

Abstract For the thorough research on coal metamorphism impact on gas adsorption capacity, this paper collected and summarized parameters of experimental adsorption isotherms, coal maceral, proximate analysis and ultimate analysis obtained from National Engineering Research Center of Coal Gas Control and related literatures at home and abroad, systematically discussed the coal rank effect on its physicochemical properties and methane adsorption capacity, in which the coal rank was shown in Vitrinite reflectance, furthermore, obtained the Semi-quantitative relationship between physicochemical properties of coal and methane adsorption capacity.

Keywords Coal rank · Methane · Physicochemical properties · Adsorption · Statistical analysis · Semi-quantitative

1 Introduction

Biological-sedimentary impact on various plants or plants in different positions under a certain geological history causes the differences of coal quality (expressed in ultimate content), coal petrology (expressed in maceral composition) and ash contents (obtained from proximate composition analysis). During the metamorphic evolution, the physicochemical properties of coal experienced a substantial change, resulting into the division of coal into subbituminous coal ($R_{o,max} < 0.5\%$), low volatile bituminous coal ($0.5\% < R_{o,max} < 0.9\%$), mid-volatile bituminous coal ($0.9\% < R_{o,max} < 1.6\%$), High bituminous coal ($1.6\% < R_{o,max} < 2.5\%$) and anthracite ($R_{o,max} > 2.5\%$). Physicochemical properties (mainly expressed in proximate composition, maceral composition and ultimate content) variation in coal leads to the adsorption characteristics difference of methane in coal, and many scholars did a lot of research on the influence factors of coal rank and physicochemical properties of coal on gas adsorption, in which the coal rank that can also influence the physicochemical properties is the main controlling factors.

Adsorption of methane in coal is an important research subject in coal mine safety and CBM exploration. Through adsorption isotherm of methane in coal, the critical desorption pressure in coal reservoir can be determined, the coalbed gas reserves can be estimated and the saturation of the CBM can be determined, finally, the extraction rate of coalbed methane can be predicted; The research for adsorption capacity of methane in coal can provide theoretical basis for industrial of CO_2-methane displacement; and it is important for the prediction of gas emission quantity and the coal and gas outbursts for studying methane adsorption in coal. In other words, Sorption of gas

✉ Yuanping Cheng
ypcheng@cumt.edu.cn

1 National Engineering Research Center of Coal Gas Control, China University of Mining and Technology, Xuzhou 221116, Jiangsu, China

2 Faculty of Safety Engineering, China University of Mining and Technology, Xuzhou 221116, Jiangsu, China

3 Institute of Mining Technology, Taiyuan University of Technology, Taiyuan 030024, Shanxi, China

4 School of Environmental and Safety Engineering, Changzhou University, Changzhou 213164, China

in coal is an ongoing and extremely important area of research to enhance coalbed methane from coal seams.

Scholars at home and abroad have already done a lot of research work in the coal rank impact on physicochemical properties of coal and coal methane adsorption characteristics (Joubert et al. 1973, 1974; Faiz et al. 1992; Levy et al. 1997; Ceglarska-Stefańska and Brzóska 1998; Laxminarayana and Crosdale 1999; Zhang and Yang 1999; Clarkson and Bustin 2000; Özgen Karacan and Okandan 2000; Fu et al. 2005; Chalmers and Marc Bustin 2007; Faiz et al. 2007a, b; Crosdale et al. 2008; Day et al. 2008; Mares and Moore 2008; Pan et al. 2010; Chen et al. 2011; Pini et al. 2011; Yao et al. 2011; Xiao and Wang 2011; Hao et al. 2012; An et al. 2013). Resulting shows that coal methane adsorption characteristics is affected by many kinds of factors, including coal rank, coal type that can be expressed in terms of many physicochemical properties, e. g. proximate analysis, maceral composition, ultimate analysis, moisture content. In the research of coal rank effect on methane adsorption, most scholars believe that with the increase of coal rank, the adsorption capacity of coal increases monotonously, while Laxminarayana (Laxminarayana and Crosdale 1999, 2002) found a 'U' relation presents between coal rank and adsorption capacity. Formerly studies on effect of moisture existence on adsorption capacity have got the following achievements: Kim et al. (2011) studied the adsorption behaviors of CH_4 on dry and wet coal and got the conclusion that the sorption capacity of CH_4 on anthracite coal was higher than those on bituminous coals at a similar condition, also, they thought that the mutual solubility between the CH_4-rich phase and aqueous phase as well as coal swelling should be considered in evaluating the sorption capacity of a wet coal seam. Cai et al. (2013a, b) investigated four coals from Northeast China and found that the data of petrographic, proximate and ultimate analyses, moisture content, ash yield had great effects on CH_4 adsorption capacity of coals. Previous studies of coal maceral effect on adsorption capacity showed that vitrinite have the higher adsorption capacity than inertinite, while some researchers hold the opposite view. Maria Mastalerz (2004) and Cai et al. (2013a, b) analyzed eight coals with similar coal rank but varying petrographic for CH_4 sorption capacity using a high-pressure adsorption isotherm technique and determined the coal quality and petrographic composition of the coals to study their relationships to the volume of CH_4 that could be sorbed into the coal. Previous studies have concluded the qualitative and partly quantitative relationship between physicochemical properties of coal and their adsorption capacity without giving variation scope of adsorption parameters (Unsworth et al. 1989; Yalçin and Durucan 1991; Reich et al. 1992; Clarkson and Bustin 1999; Mastalerz et al. 2009; Charrière et al. 2010; Yao and Liu 2012).

Different from the former research of using Limited quantity of coal samples, focusing on a certain coal mine, or a certain influential factor, data obtained from the National Engineering Research Center of Coal Gas Control (NERC) and the related literatures at home and abroad are collected to discuss the effect of physicochemical properties of coal on methane adsorption capacity by observing the changing rule of physicochemical properties of coal and methane adsorption capacity with coal rank separately. Whereas, physicochemical data are scattered as the macromolecular structure and difference of environmental and metamorphic factors for the formation of a certain coal are complexity. Besides, because of the different research aims in different literatures, not all the data can meet requirements of this paper, then, we did some data transmission work to obtain a Semi-quantitative result and to strengthen the understanding of the factors influencing the adsorption capacity.

2 Methods

For the thorough research on coal metamorphism impact on gas adsorption capacity, this paper collected and summarized parameters of experimental adsorption isotherms, coal maceral, proximate composition and ultimate contents obtained from the National Engineering Research Center of Coal Gas Control (NERC) and related literatures at home and abroad, systematically discussed the coal rank impact on its physicochemical properties and methane adsorption capacity, in which the coal rank was shown in maximum Vitrinite reflectance $R_{o,max}$. In this paper, the changing rules of physicochemical properties of coal and methane adsorption capacity with coal rank were observed separately and then the relationships between physicochemical properties of coal and adsorption capacity were obtained.

Proximate analysis of coal (Mahajan and Walker 1971; Bhattacharyya 1972; Reucroft and Patel 1986; Friesen and Mikula 1988; Banerjee 1988, Barker-Read and Radchenko 1989; Yalçin and Durucan 1991; DeGance et al. 1993; Chaback et al. 1996; Clarkson et al. 1997; Bustin and Clarkson 1998; Özgen Karacan and Okandan 2000; Laxminarayana and Crosdale 2002; Wang and Takarada 2003; Bae and Bhatia 2006; Qin et al. 2007; Saghafi et al. 2007; Dutta et al. 2008; Yu et al. 2008a, b, c; Pini et al. 2009; Pone et al. 2009; Battistutta et al. 2010; Gensterblum et al. 2010; He et al. 2010; Pan et al. 2010; Kim et al. 2011; Zheng 2012; Wang 2012; Jiang et al. 2012; Kutchko et al. 2013; An et al. 2013; Hao et al. 2013; Xiao et al. 2016) consists of moisture, ash, volatile, fixed carbon. The

widely-used index are: air dried basis (ad), dry basis (d), dry ash-free basis (daf). To avoid the effects of inorganic material of moisture and ash, we applied the index of dry ash-free basis volatile (V_{daf}). Similarly, to avoid the effects of moisture, we applied the index of dry basis ash (daf). The Moisture and Fixed carbon use the air dried basis index, as the index employed by different articles that are different with this paper, we adopted the Eqs. (1)–(5) for transformation:

$$V_{daf} = \frac{100V_{ad}}{100 - M_{ad} - A_{ad}} \quad (1)$$

$$V_{daf} = \frac{100V_{d}}{100 - A_{ad}} \quad (2)$$

$$A_{d} = \frac{100A_{ad}}{100 - M_{ad}} \quad (3)$$

$$F_{cad} = 100 - M_{ad} - A_{ad} - V_{ad} \quad (4)$$

$$F_{cadf} = 100 - V_{daf}. \quad (5)$$

The maceral (Ceglarska-Stefańska and Brzóska 1998; Crosdale et al. 1998; Laxminarayana and Crosdale 2002; Busch et al. 2003; Mastalerz et al. 2004; Chang et al. 2006; Busch et al. 2006; Qin et al. 2007; Majewska and Ziętek 2007; Siemons et al. 2007; Chang et al. 2008; Day et al. 2008; Mazumder and Wolf 2008; Pone et al. 2009; Majewska et al. 2009; Radliński et al. 2009; Battistutta et al. 2010; Gensterblum et al. 2010; He, et al. 2010; Day et al. 2011; Kim et al. 2011; Jiang et al. 2012; Maphala and Wagner 2012; An et al. 2013; Cai et al. 2013a, b; Lin et al. 2013; Dutka et al. 2013; Xiao et al. 2016) include Vitrinite, Inertinite, Exinite. The common indicators are: moist mineral matter basis, and moist mineral matter-free basis (mmf). As the indexes employed by literatures at home and abroad are not consistent, we adopted the mmf index in this paper and used the Eq. (6) for transformation:

$$X_{daf} = \frac{100X_{mineral}}{100 - Mineral}, \quad X = Vitrinite, Inertinite, Exinite. \quad (6)$$

Ultimate analysis specifies the elements of carbon, hydrogen, nitrogen, oxygen and sulphur (Gan et al. 1972; Joubert et al. 1973; Nandi and Walker 1975; Nelson et al. 1980; Reucroft and Yang and Saunders 1985; Reucroft and Patel 1986; Banerjee 1988; Friesen and Mikula 1988; Giuliani et al. 1991; DeGance et al. 1993; Chaback et al. 1996; Wang and Takarada 2003; Fitzgerald et al. 2005; Chang et al. 2006; Qin et al. 2007; Siemons et al. 2007; Chang et al. 2008; Majewska et al. 2009; Radliński et al. 2009; Pone et al. 2009; Battistutta et al. 2010; Gensterblum et al. 2010; Kim et al. 2011; Hao et al. 2012, 2013; Lin et al. 2013). Widely-used indexes for ultimate analysis are: dry ash-free basis, air dried basis. To avoid moisture effect, we applied dry ash-free basis index in this paper. As the index employed by different articles that are different with this paper, we adopted the Eq. (7) for transformation:

$$X_{daf} = \frac{100X_{ad}}{100 - A_{ad} - M_{ad}}, \quad X = C, H, O, N, S. \quad (7)$$

3 Coal rank effect on adsorption capacity

The following Langmuir adsorption isotherm pattern is used:

$$Q = \frac{abP}{1 + bP} \quad (8)$$

where, Q is the adsorption capacity under an equilibrium of P, m^3/t, a is limit monolayer adsorption capacity, m^3/t, b is pressure constant, MP^{-1}.

3.1 Coal rank effect on adsorption constant a_{daf}

To avoid the effects of moisture, ash on methane adsorption capacity, we adopted the dry ash-free basis index to analyze the limit monolayer adsorption capacity a, expressed in a_{daf}. As the index employed by different articles that are different with this paper, we adopted the Eq. (9) for transformation:

$$a_{daf} = \frac{100a_{ad}}{100 - M_{ad} - A_{ad}}. \quad (9)$$

The statistical analysis of the relationship between limit monolayer adsorption capacity (a_{daf}) and vitrinite reflectance $R_{o,max}$ was shown in Fig. 1.

Adsorption isotherm results (Fig. 1) indicate that Langmuir volumes a_{daf} follows a upwards, discrete, second-order polynomial trends with increasing coal rank, which is consistent with the conclusion of Levy et al. 1997. Figure 1 shows that the range of a_{daf} for Lignite/subbituminous is 13–34 m^3/t, for low volatile bituminous is 8–48 m^3/t, for middle volatile bituminous is 4–52 m^3/t, for high volatile bituminous is 6–60 m^3/t and for semi-anthracite/anthracite is 16–50 m^3/t. Besides, upper and lower limits exists in the relationship between a_{daf} and $R_{o,max}$, the upper and lower curves are separately represented in the equations of $a_{daf,max} = 13.4R_{o,max} - 25.01R_{o,max} + 57.72$ and $a_{daf,min} = 1.014R^2_{o,max} - 0.014R_{o,max} + 7.18$, the corresponding average curve is: $a_{daf,avr} = 9.3135R^2_{o,max} - 22.2865R_{o,max} + 32.673$, from the corresponding average curve, we can see that the a_{daf} decrease as the coal rank increase in the range of $R_{o,max} = 0.4\% - 1.196\%$, while in the range of $R_{o,max} = 1.196\% - 7\%$, the a_{daf} increase as the coal rank increase. The reason is that the porosity of the

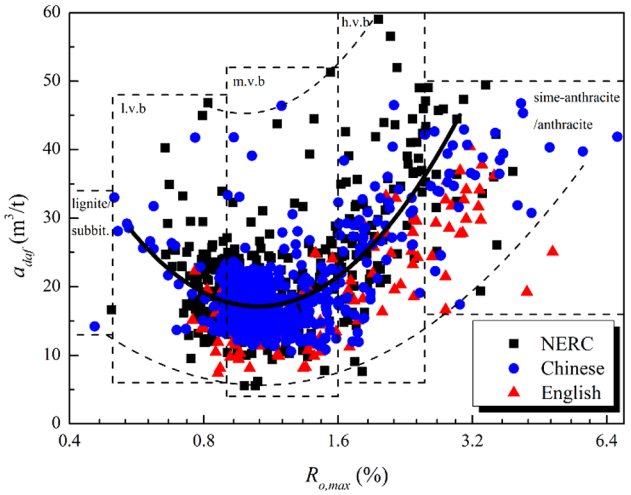

Fig. 1 Value of adsorption constant a_{daf} versus vitrinite reflectance $R_{o,max}$. (Data size: NERC-290, Chinese (Zhang and Yang 1999; Fu et al. 2002; Zhang et al. 2004; Fu et al. 2005; Su et al. 2005; Su et al. 2006; Chen et al. 2008; Fu et al. 2008; Zhang and Sang 2008; Wang et al. 2008; Yu et al. 2008a; Chen et al. 2008; Jiang 2009; Zhang and Sang 2009; Yang et al. 2009; Ren 2010; Tian et al. 2010; Zhang et al. 2011; Zhang Jun-fan and Liang Wen-qing 2011; Zheng 2012; Gao 2012; Ma et al. 2014; Zhang et al. 2014)-173; English(Joubert et al. 1973; Yalçin and Durucan 1991; Beamish and O'Donnell 1992; DeGance et al. 1993; Chaback et al. 1996; Bustin and Clarkson 1998; Nodzeński 1998; Faiz et al. 2007a, b; Yu et al. 2008a, b, c; Xiao and Wang 2011)-103)

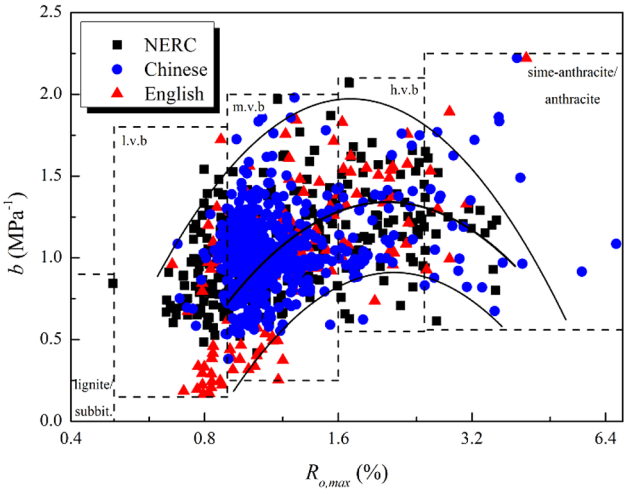

Fig. 2 Value of adsorption constant b versus vitrinite reflectance $R_{o,max}$. (Data size: NERC-290, Chinese (Zhang and Yang 1999; Su et al. 2006; Ma et al. 2008; Yang et al. 2009; Tian et al. 2010; Zheng 2012; Gao 2012; Ma et al. 2014; Pan and Xu 2015; Xu and Pan 2015)-217, English (Joubert et al. 1973; Yalçin and Durucan 1991; DeGance et al. 1993; Chaback et al. 1996; Bustin and Clarkson 1998; Nodzeński 1998; Faiz et al. 2007a, b; Yu et al. 2008a, b, c)-153)

low rank coal is larger, resulting in the stronger adsorption capacity. With the increase of buried depth, adsorption capacity decrease with the compaction of larger pores because of the increasing overburden pressure. With the enhancement of maturity, adsorption capacity increase again with the increasing pore volume and specific area because of the increasing reservoir pressure coefficient.

3.2 Coal rank effect on adsorption constant b

To analyze the relationship between Langmuir constant b and vitrinite reflectance $R_{o,max}$, we did the Fig. 2.

Figure 2 indicates that constant b follows a downward, discrete, second-order polynomial trends with vitrinite reflectance $R_{o,max}$, which is not related to coal type. Constant b for the Lignite/subbituminous is between 0 and 0.9 MPa^{-1}, for low volatile bituminous is between 0.15 and 1.8 MPa^{-1}, for middle volatile bituminous is between 0.25 and 2 MPa^{-1}, for high volatile bituminous is between 0.55 and 2.1 MPa^{-1} and for semi-anthracite/anthracite is between 0.56 and 2.25 MPa^{-1}. The variation range is between the upper and lower curves represented in the equations of $b_{max} = -0.16R_{o,max}^2 + 0.74467R_{o,max} + 0.899$ and $b_{min} = -0.2687R_{o,max}^2 + 1.321R_{o,max} - 0.6754$, and the corresponding average curve is: $b_{avr} = -0.43019R_{o,max}^2 + 0.90056R_{o,max} + 0.86969$, from the corresponding average curve, we can see that the constant b increase as the coal rank increase in the range of $R_{o,max} = 0.4\%-1.05\%$; while in the range of $R_{o,max} = 1.05\%-7\%$, The constant b decreases as the coal rank increases. And from the upper curve, we can see that the constant b reaches max at $R_{o,max} = 1.765\text{MP}^{-1}$.

3.3 Coal rank effect on adsorption Q_{daf}

The Eq. (10) was employed to obtain dry ash-free basis gas content Q_{daf}:

$$Q_{daf} = \frac{a_{daf}bP}{1+bP} \tag{10}$$

Set the equilibrium pressure in Eq. (10) as 1 MPa, we can obtain the corresponding gas content Q_{daf}. Figure 3 shows the relationship between Q_{daf} at 1 MPa and the vitrinite reflectance $R_{o,max}$.

Figure 3 shows that Q_{daf} for the Lignite/subbituminous is between 0 and 8 m^3/t, for low volatile bituminous is between 3 and 24 m^3/t, for middle volatile bituminous is between 5 and 29 m^3/t, for high volatile bituminous is between 6 and 36 m^3/t and for semi-anthracite/anthracite is between 8 and 30 m^3/t. The variation range is between the upper and lower curves represented in the equations of $Q_{daf,max} = -4.9549R_{o,max}^2 + 13.263R_{o,max} + 27.6$ and $Q_{daf,min} = 2.847R_{o,max}^2 - 1.84R_{o,max} + 4.97$.

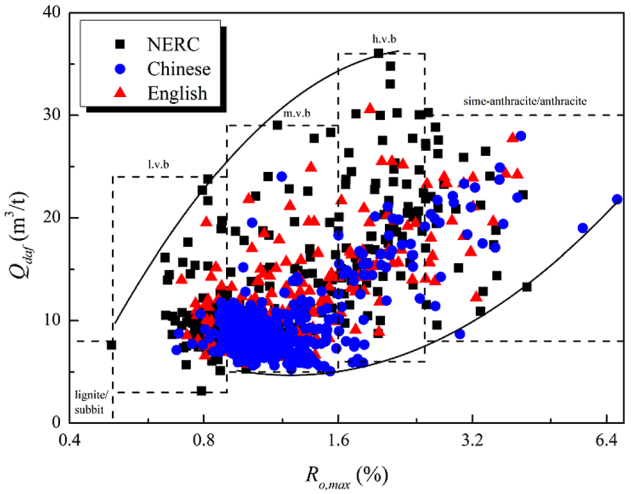

Fig. 3 Value of adsorption constant Q_{daf} versus vitrinite reflectance $R_{o,max}$. (Data size: NERC-290, Chinese (Yu et al. 2005; Zhang 2007; Zheng 2012; Zou et al. 2013; Liu et al. 2015; Yue et al. 2016)-217, English(Joubert et al. 1973; Yalçin and Durucan 1991; DeGance et al. 1993; Chaback et al. 1996; Bustin and Clarkson 1998; Nodzeński 1998; Yu et al. 2008a, b, c)-153)

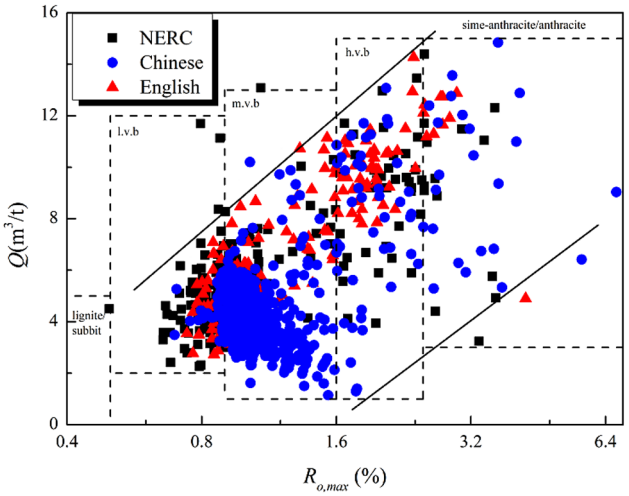

Fig. 4 Value of adsorption constant Q versus vitrinite reflectance $R_{o,max}$. (Data size: NERC-290, Chinese (Yu et al. 2008a; Ma et al. 2008; Jiang 2009; Tian et al. 2010; Zhang et al. 2011; Zheng 2012; Gao 2012; Ma et al. 2014; Xu and Pan 2015)-117, English(Joubert et al. 1973; Yalçin and Durucan 1991; DeGance et al. 1993; Chaback et al. 1996; Nodzeński 1998; Yu et al. 2008a, b, c)-153)

3.4 Coal rank effect on gas content of raw coal

Taken into account the factors influence the actual gas content, we applied the Eq. (11) (Chen et al. 2010; Gao 2012) for transformation:

$$Q = Q_{daf}\frac{100 - A_{ad} - M_{ad}}{100}\frac{1}{1 + 0.31M_{ad}} \quad (11)$$

where, A_{ad} is the air dried basis ash, %; M_{ad} is the air dried basis moisture, %; Q_{daf} is the dry ash-free basis gas content, m^3/t; Q is the gas content of raw coal, m^3/t.

Figure 4 shows the relationship between Q at 1 MPa and the vitrinite reflectance $R_{o,max}$:

From Fig. 4, it can be concluded that the Q increases with the coal rank. The formula between Q and $R_{o,max}$ was shown in Eq. (12):

$$Q = k_Q R_{o,max} + b_Q \quad (12)$$

where, Q is the gas content at the equilibrium pressure of 1 MPa; k_Q and b_Q are the coefficients in Eq. (12), and $k_Q > 0$.

Figure 4 shows that Q for the Lignite/subbituminous is between 0 and 5 m^3/t, for low volatile bituminous is between 2 and 12 m^3/t, for middle volatile bituminous is between 1 and 13 m^3/t, for high volatile bituminous is between 1 and 15 m^3/t and for semi-anthracite/anthracite is between 3 and 15 m^3/t. The variation range is between the upper and lower curves represented in the equations of $Q_{max} = 4.49R_{o,max} + 8.9386$ and $Q_{min} = 3.9266R_{o,max} - 2.545$. Comparing with Fig. 3, it can be seen that the value of Q is smaller than Q_{daf} because of the Physico-chemical difference.

4 Analysis of factors effect on adsorption capacity of coal

4.1 Proximate composition effect on adsorption capacity

Proximate analysis is usually used to define the chemical composition of coals. With proximate analysis, the substances of moisture, ash, volatile matter and fixed carbon in the coal content are determined as weight percent. In the four indexes, moisture and ash represents the inorganic material, while volatile and fixed carbon represents the organic material.

4.1.1 Volatile content effect on adsorption capacity

Commonly used indexes for Volatile are: dry air basis volatile (V_{ad}), dry basis volatile (V_d), dry ash-free basis volatile (V_{daf}) and Received basis volatile (V_{ar}). To avoid the effect of moisture, ash on volatile matter, the volatile matter was determined by using dry ash-free basis on weight percent. Figure 5 shows the relationship between volatile (V_{daf}) and vitrinite reflectance ($R_{o,max}$).

Figure 5 shows the relationship between Dry ash-free basis volatile V_{daf} and Vitrinite reflectance $R_{o,max}$ expressed in Eq. (13):

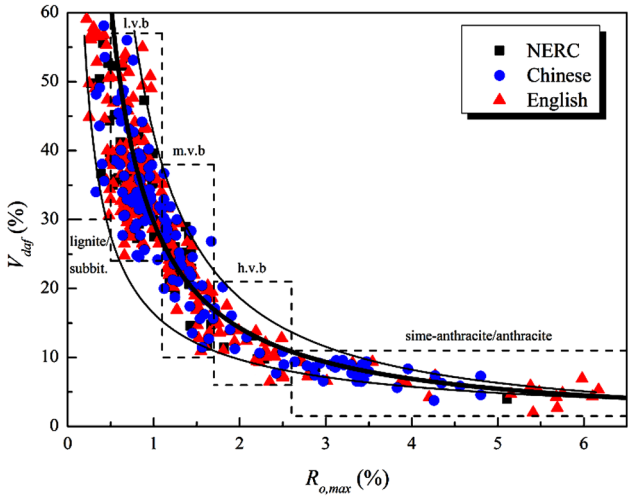

Fig. 5 Variation of V_{daf} with vitrinite reflectance $R_{o,max}$. (Data size: NERC-189, Chinese (Yu et al. 2004; Chang et al. 2006; Qin et al. 2007; Chang et al. 2008; Chen et al. 2010; Hao et al. 2012; Zheng 2012; Jiang et al. 2012; Gao 2012; Lin et al. 2013; Li et al. 2013; Xiao et al. 2016)-135, English, (Mahajan and Walker 1971; Joubert et al. 1973; Yalçin and Durucan 1991; DeGance et al. 1993; Chaback et al. 1996; Nodzeński 1998; Wang 2012)-171)

$$V_{daf} = k_{vdaf} R_{o,max}^{b_{vdaf}} \tag{13}$$

where, V_{daf} is the dry ash-free basis volatile; k_{vdaf}, b_{vdaf} are the coefficients in Eq. (13), and $k_{vdaf} > 0$, $b_{vdaf} < 0$.

The first and order derivative are separately shown in Eqs. (14) and (15):

$$V'_{daf} = k_{vdaf} b_{vdaf} R_{o,max}^{b_{vdaf}-1} \tag{14}$$

$$V'_{daf} = k_{vdaf} b_{vdaf} (b_{vdaf} - 1) R_{o,max}^{b_{vdaf}-2} \tag{15}$$

As $k_{vdaf} > 0$, $b_{vdaf} < 0$, the first derivative (Eq. 14) of Eq. (13) is always less than zero, while the second derivative (Eq. 15) is always greater than zero. According to the properties of function, it can be concluded that Eq. (13) exhibits depression, power-decreasing type. In conclusion, volatile decrease with the increase of coal rank, and compared with the higher coal rank, the volatile at the low metamorphic grade has a much more significantly decrease. The reason is that Volatile matter are mainly small molecular compound broke from unsaturated group in the side-chain of fat and the oxygen-containing functional groups that decreases with the coal rank.

Figure 5 shows that Dry ash-free basis volatile V_{daf} for the Lignite/subbituminous is larger than 30%, for low volatile bituminous is between 25% and 58%, for middle volatile bituminous is between 10% and 38%, for high volatile bituminous is between 5% and 20% and for semi-anthracite/anthracite is smaller than 10%. The variation range is between the upper and lower curves represented in the equations of $V_{daf,max} = 42.39 R_{o,max}^{-1.183}$ and $V_{daf,min} = 16.39 R_{o,max}^{-0.756}$, and the corresponding average curve is $V_{daf,avr} = 29.63 R_{o,max}^{-1.05}$. For low metamorphic bituminous coal, the vitrinite reflectance changes smaller with scattered volatile V_{daf} content falling in 25%–58%;

Features for the mid volatile bituminous coal are with the wide range of volatile matter content falling in 10%–38% because of the complex generation environment and constitution of coal rock; volatile matter content of the high volatile bituminous coal falls in 5%–20%; while the volatile matter content in anthracite is the lowest, less than 10%.

Combing Eqs. (12) and (13), the quantitative formula of Eq. (16) can be obtained:

$$Q = k_Q \left(\frac{V_{daf}}{k_{vdaf}} \right)^{\frac{1}{b_{vdaf}}} + b_Q \tag{16}$$

$$Q' = \frac{k_Q}{b_{vdaf} k_{vdaf}^{\frac{1}{b_{vdaf}}}} V_{daf}^{\frac{1}{b_{vdaf}}-1} \tag{17}$$

$$Q'' = \frac{k_Q \left(\frac{1}{b_{vdaf}} - 1 \right)}{b_{vdaf} k_{vdaf}^{\frac{1}{b_{vdaf}}}} V_{daf}^{\frac{1}{b_{vdaf}}-2} \tag{18}$$

As $\frac{1}{b_{vdaf}} < 0$, $k_Q > 0$, $k_{vdaf} > 0$, so $k_{vdaf}^{\frac{1}{b_{vdaf}}} > 0$,the first derivative (Eq. 17) of Eq. (16) is always less than zero, while the second derivative (Eq. 18) is always greater than zero, thus, it can be concluded that Eq. (16) exhibits depression, power-decreasing type, it can be concluded that gas content in raw coal decreases with the increase of dry ash-free basis volatile V_{daf}, and the gas content in raw coal at the low metamorphic grade has a much more significantly decrease.

4.1.2 Moister content effect on adsorption capacity

Moisture in coal generally divided into inherent moisture and external moisture. Inherent moisture existing in the underdeveloped pore is from the plant turned to coal; external moisture existing in the well-developed pore and crack is form the process of mining and transport. The moisture was determined using air dried basis on weight percent, expressed in M_{ad} with the value equal to inherent moisture. Figure 6 shows the relationship between air dried basis moisture (M_{ad}) and vitrinite reflectance ($R_{o,max}$).

Figure 6 show that moisture in coal decreases with the coal rank, and the functional relationship between inherent moisture M_{ad} and vitrinite reflectance $R_{o,max}$ is shown in Eq. (19):

$$M_{ad} = k_{mad} \exp(R_{o,max}/c_{mad}) + b_{mad} \tag{19}$$

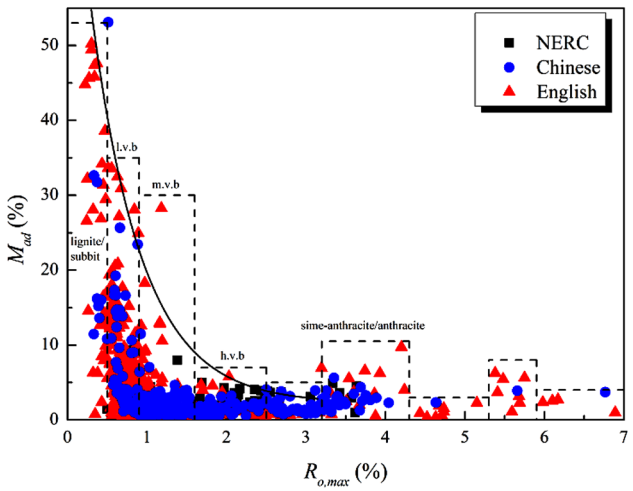

Fig. 6 Variation of M_{ad} with vitrinite reflectance $R_{o,max}$. (Data size: NERC-189, Chinese (Yu et al. 2004; Chang et al. 2006; Qin et al. 2007; Chang et al. 2008; Hao et al. 2012; Zheng 2012; Jiang et al. 2012; Gao 2012; Lin et al. 2013; Li et al. 2013; Xiao et al. 2016)-169, English(Allardice and Evans 1971; Mahajan and Walker 1971; Bhattacharyya 1972; Joubert et al. 1973; Reucroft and Patel 1986; Banerjee 1988; Barker-Read and Radchenko 1989; Yalçin and Durucan 1991; Ciembroniewicz and Marecka 1993; DeGance et al. 1993; Chaback et al. 1996; Clarkson et al. 1997; Crosdale et al. 1998; Bustin and Clarkson 1998; Friesen and Mikula 1988; Özgen Karacan and Okandan 2000; Laxminarayana and Crosdale 2002; Busch et al. 2003; Wang and Takarada 2003; Weishauptová et al. 2004; Mastalerz et al. 2004; Fitzgerald et al. 2005; Hildenbrand et al. 2006; Bae and Bhatia 2006; Dai et al. 2006; Busch et al. 2006; Faiz et al. 2007a, b; Saghafi et al. 2007; Majewska and Ziętek 2007; Faiz et al. 2007a, b; Astashov et al. 2008; Yu et al. 2008a, b, c; Zhang 2008; Dutta et al. 2008; Day et al. 2008; Pini, et al. 2009; Kędzior 2009; Pone et al. 2009; Majewska et al. 2009; Majewska et al. 2010; Battistutta et al. 2010; Gensterblum et al. 2010; Pan et al. 2010; He, et al. 2010; Jin et al. 2010; Kim et al. 2011; Day et al. 2011; Wang 2012; An et al. 2013; Dutka et al. 2013; Hao et al. 2013; Kutchko et al. 2013)-258)

where M_{ad} is air dried basis inherent moisture, %; k_{mad}, c_{mad}, b_{mad} are coefficients of Eq. (19), and $c_{mad} < 0$, $k_{mad} > 0$.

The first and order derivative are separately shown in Eqs. (20) and (21):

$$M'_{ad} = \frac{k_{mad}}{c_{mad}} \exp\left(R_{o,max}/c_{mad}\right) \tag{20}$$

$$M''_{ad} = \frac{k_{mad}}{c^2_{mad}} \exp\left(R_{o,max}/c_{mad}\right) \tag{21}$$

As $c_{mad} < 0$, $k_{mad} > 0$, the first derivative (Eq. 20) of Eq. (19) is always less than zero, while the second derivative (Eq. 21) is always greater than zero, thus, it can be concluded that Eq. (19) exhibits depression, exponent-decreasing type, it can be concluded that inherent moisture decreases with the coal rank and has a much more significantly decrease at the low metamorphic grade. From Fig. 6, it can be seen that the maximum of moisture are generally less than the values in the curves of $M_{ad,max} = 2.217 + 83.84 \exp\left(R_{o,max}/-0.64\right)$. The ranges of inherent moisture in subbituminous coal are from 0% to 55%, in low volatile bituminous coal with lots of pores are from 0% to 35%, in mid volatile bituminous coal with lots of hydrophobic fused ring structure in organic structure are from 0% to 30%, in high volatile bituminous coal are from 0% to 8%, in anthracite are from 0% to 10%. Besides, at the range of 3.2%–4.2% and 5.2%–5.9% had an increasing zone, and the corresponding inherent moisture are separately 0%–10% and 0%–9%, the possibly reason maybe the existence of the aphanitic structure.

Reasons for the changing trend of inherent moisture are summarized below: (1) adsorption character of pore surface on moisture, the higher internal surface area is the high moisture absorbed. (2) The more Polarity oxygen-containing groups in coal, the larger inherent moisture content. (3) The surface area and Polarity oxygen-containing groups decrease with the increase of coal rank, resulting in the decease of inherent moisture.

Combing Eqs. (12) and (19), Eq. (22) can be obtained:

$$Q = k_Q c_{mad} \ln\left(\frac{M_{ad} - b_{mad}}{k_{mad}}\right) + b_Q \tag{22}$$

$$Q' = \frac{k_Q c_{mad}}{M_{ad} - b_{mad}} \tag{23}$$

$$Q'' = \frac{-k_Q c_{mad}}{(M_{ad} - b_{mad})^2} \tag{24}$$

As $k_Q > 0$, $c_{mad} < 0$, $k_{mad} > 0$, the first derivative (Eq. 23) of Eq. (22) is always less than zero, while the second derivative (Eq. 24) is always greater than zero, thus, it can be concluded that Eq. (22) exhibits depression, logarithmic-decreasing type, that is the gas content Q in raw coal has a negative relationship with the inherent moisture M_{ad}. Also, it can be concluded from Eq. (22) that gas content Q in raw coal has a much more significantly decrease at the low inherent moisture grade. The reasons for the effects of moisture content on adsorption of coal are generally as follow: (1) Effective adsorption sites at the pore surface are limited, the more the moisture is, the more adsorption sites can be occupied, then the less adsorption sites can be used for methane. (2) The preferential adsorption of moisture results in the decreased gas content. (3) Due to the adsorption of methane in micro-pore with high capillary pressure and strong self-priming capacity, the moisture in coal can restrict the adsorption of methane. (4) Existing of moisture can cause matrix shrinkage of coal resulting in the decrease of gas content.

4.1.3 Ash content effect on adsorption capacity

Ash is the remaining residue after full combustion of coal, and almost all of it comes from minerals. Usually, the ash content is proportional to the mineral content. Ash is not an inherent component of coal but a very different matter from minerals in coal. First, the ash content is lower than corresponding mineral content, and then their composition is changed, Minerals at high temperature after decomposition, oxidation, combining chemical reaction can turn into ash. Because of the changed moisture in the air dried coal with the change of air humidity, the ash content of the coal sample changed. But in terms of absolute dry coal, the ash content is the same. Thus, dry basis ash A_d is used in the actual. Figure 7 shows the relationship between dry basis ash (A_d) and vitrinite reflectance ($R_{o,max}$).

Figure 7 shows that the ash content value is more dispersed. This is because the ash is affected largely by the geological evolution conditions; Ash showed a decreasing trend with the increase metamorphism degree. The maximum ash value does not exceed the curve shown in this formula: $A_{d,max} = -8.657R_{o,max} + 68.435$. The ranges of ash content in subbituminous coal are from 0% to 70%, in low volatile bituminous coal are from 0% to 62%, in mid volatile bituminous coal are from 0% to 59%, in high volatile bituminous coal are from 0% to 49%, in anthracite are from 0% to 43%.

Existence of ash in coal has adverse effects on coal adsorption capacity. The effect mechanism of ash on coal adsorption is mainly: (1) the first is based on the principle of similar compatibility, the properties of methane is similar to the organic matter with weak polarity and better adsorption character, but ash is mostly inorganic with weak adsorption capacities, the presence of ash reduced the adsorption content of methane in coal; (2) the presence of silica, iron, calcium and magnesium and other group, especially the presence of metal elements resulting in the basal cementation tendency of rock, and the increasing cements will block the coal pore and fissure, reducing the porosity of coal, resulting in the decreasing of adsorption capacity of methane in coal. The comprehensive function of the two aspects reduces the ability of organic matter to adsorb methane in coal, In view of this, in the evaluation of ash effect on adsorption of coal, authors should consider not only the impact of ash content, but also consider the state of ash adsorption sites.

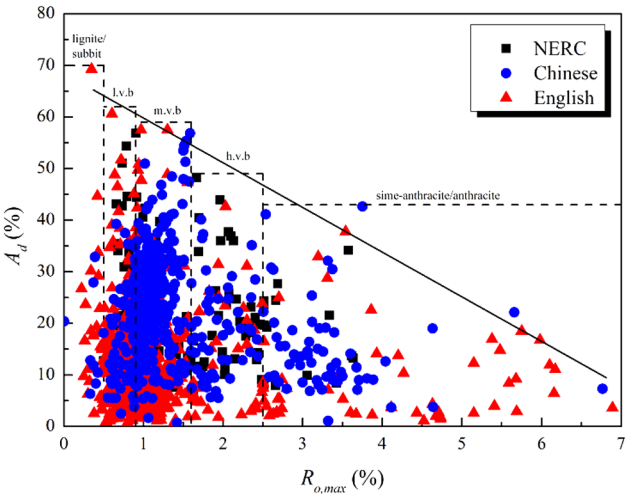

Fig. 7 Variation of A_d with vitrinite reflectance $R_{o,max}$. (Data size: NERC-189, Chinese (Yu et al. 2004; Chang et al. 2006; Qin et al. 2007; Chang et al. 2008; Hao et al. 2012; Zheng 2012; Gao 2012; Jiang et al. 2012; Li et al. 2013; Lin et al. 2013; Xiao et al. 2016)-268, English, (Mahajan and Walker 1971; Joubert et al. 1973; Yalçin and Durucan 1991; DeGance et al. 1993; Chaback et al. 1996; Bustin and Clarkson 1998; Nodzeński 1998; Hildenbrand et al. 2006; Faiz et al. 2007a, b; Faiz et al. 2007; Yu et al. 2008a, b, c; Gensterblum et al. 2010; Taraba 2011; Wang 2012)-297)

4.1.4 Fixed carbon content effect on adsorption capacity

Carbon Fixed is the residue after subtracting the ash from the coke residue determined after the measurement of volatile in coal, In fact, it is the pyrolysis product produced by the organic matter under certain heating conditions, and it is a part of the coke residue. Carbon Fixed is mainly composed of carbon elements, some of the hydrogen, sulfur and a small amount of oxygen and nitrogen elements. In proximate analysis, Fixed carbon always expressed in Fc_{ad}, Fig. 8 shows the relationship between Fixed carbon (Fc_{ad}) and Vitrinite reflectance ($R_{o,max}$).

Figure 8 shows the relationship between air dried basis Fixed carbon and vitrinite reflectance:

$$Fc_{ad} = k_{Fcad}\exp(c_{Fcad}R_{o,max}) + b_{Fcad} \tag{25}$$

where, Fc_{ad} is air dried basis fixed carbon, %; k_{Fcad}, c_{Fcad}, b_{Fcad} are coefficients of Eq. (25),and $c_{Fcad} < 0$, $k_{Fcad} < 0$.

The first and order derivative are separately shown in Eqs. (26) and (27):

$$Fc'_{ad} = \frac{k_{Fcad}}{c_{Fcad}}\exp\left(R_{o,max}c_{Fcad}\right) \tag{26}$$

$$Fc''_{ad} = \frac{k_{Fcad}}{c^2_{Fcad}}\exp(R_{o,max}c_{Fcad}) \tag{27}$$

As $c_{Fcad} < 0$, $k_{Fcad} < 0$, the first derivative (Eq. 26) of Eq. (25) is always larger than zero, while the second derivative (Eq. 27) is always less than zero, thus, it can be concluded that Eq. (25) exhibits up-convex, power-decreasing type, it can be concluded that Fixed carbon increases with the increase of coal rank, and at low metamorphic stage, Fixed carbon content increases greatly.

Figure 8 shows that with the increase of coal rank, the fixed carbon content exists the upper and lower curves

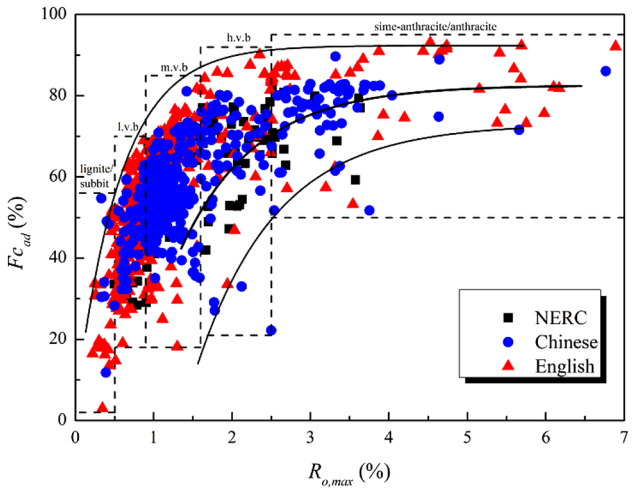

Fig. 8 Variation of Fc_{ad} with vitrinite reflectance $R_{o,max}$. (Data size: NERC-189, Chinese (Yu et al. 2004; Chang et al. 2006; Qin et al. 2007; Chang et al. 2008; Hao et al. 2012; Zheng 2012; Jiang et al. 2012; Gao 2012; Li et al. 2013; Lin et al. 2013)-266, English (Mahajan and Walker 1971; Bhattacharyya 1972; Joubert et al. 1973; Joubert et al. 1974; Yang and Saunders 1985; Banerjee 1988; Friesen and Mikula 1988; Barker-Read and Radchenko 1989; Yalçin and Durucan 1991; DeGance et al. 1993; Chaback et al. 1996; Clarkson et al. 1997; Crosdale et al. 1998; Bustin and Clarkson 1998; Özgen Karacan and Okandan 2000; Laxminarayana and Crosdale 2002; Wang and Takarada 2003; Weishauptová et al. 2004; Fitzgerald et al. 2005; Bae and Bhatia 2006; Dai et al. 2006; Saghafi et al. 2007; Majewska and Ziętek 2007; Faiz et al. 2007a, b; Siemons et al. 2007; Yu et al. 2008a, b, c; Zhang 2008; Dutta et al. 2008; Day et al. 2008; Majewska et al. 2009; Kędzior 2009; Pini et al. 2009; Pone et al. 2009; Battistutta et al. 2010; Pan et al. 2010; Gensterblum et al. 2010; He et al. 2010; Kim et al. 2011; Day et al. 2011; Wang 2012; Dutka et al. 2013; An et al. 2013; Hao et al. 2013; Kutchko et al. 2013)-268)

expressed in the following equations:$Fc_{ad,max} = 92.3433 - 88.918\exp(-1.7628R_{o,max})$ and $Fc_{ad,min} = 73.01726 - 273.61127\exp(-0.9814R_{o,max})$, The corresponding average curve is as follow: $Fc_{ad,avr} = 82.57758 - 162.60685\exp(-1.03532R_{o,max})$,besides, The ranges of fixed carbon content in subbituminous coal are from 2% to 56%, in low volatile bituminous coal are from 18% to 70%, in mid volatile bituminous coal are from 18% to 85%, in high volatile bituminous coal are from 21% to 92%, in anthracite are from 50% to 95%.

Combing Eqs. (25) and (12):

$$Q = \frac{k_Q}{c_{Fcad}} \ln\left(\frac{Fc_{ad} - b_{Fcad}}{k_{Fcad}}\right) + b_Q \tag{28}$$

$$Q' = \frac{k_Q/c_{Fcad}}{Fc_{ad} - b_{Fcad}} \tag{29}$$

$$Q'' = \frac{-k_Q/c_{Fcad}}{(Fc_{ad} - b_{Fcad})^2} \tag{30}$$

As $k_Q > 0$, $c_{Fcad} < 0$, $k_{Fcad} < 0$,the first derivative (Eq. 29) of Eq. (28) is always greater than zero, while the second derivative (Eq. 30) is always greater than zero, thus, it can be concluded that Eq. (28) exhibits depression, logarithmic-increasing type. The increase of carbon Fixed content has a reinforcing effect on the adsorption capacity of raw coal, and in the low carbon Fixed content stage, the amount adsorbed gas in coal decreases significantly.

The research shows that with the increase of carbon fixed content, the specific surface area and pore volume increases, The surface morphology of coal shows that the particles become small, the size is uniform, the arrangement is more orderly, the space for the adsorption of methane in coal is increasing, and finally the coal methane adsorption capacity is enhanced.

4.2 Maceral composition effect on adsorption capacity of raw coal

The maceral types in coals are mainly vitrinite, inertinite, rare exinite and little mineral matter. Differences of maceral groups in composition and structure resulted in the different characteristics, and these characteristics directly decides the macroscopic properties of coal. Branch of various group experienced different changes, resulting in the difference of chemical composition, molecular structure and pore. Gelation and wire charring effect is different, resulting in different degree of plant tissue preservation. In the process of coal metamorphism, the difference of hydrocarbons, volatile matter content resulted in the different pore growth degree. Thus, there is difference in the adsorption capacity of macerals.

It is generally believed that adsorption capacity of exinite is the lowest, and as the main components of the organic maceral, the vitrinite and inertinite have the strong adsorption capacity with the increase in the metamorphism degree, the two show the shift tendency, indicating that inertinite gradually evolved into vitrinite. Therefore, in this paper, we mainly study the relationship between vitrinite and inertinite with the metamorphism degree, in order to get the effect of the two matters on adsorption capacity.

4.2.1 Vitrinite content effect on adsorption capacity

Vitrinite is the main maceral in coal, and is the jelly-like substance formed from the wood cellulose of plant tissue under the gel conditions. According to the intact degree of cell structure and cell forms, size and other characteristics, the most common vitrinite components are divided into anthraxylon, homocollinite and degradinite. Figure 9 represents the relationship between vitrinite and vitrinite reflectance ($R_{o,max}$).

Figure 9 shows that, the relationship between vitrinite and vitrinite reflectance is expressed as Eq. (31)

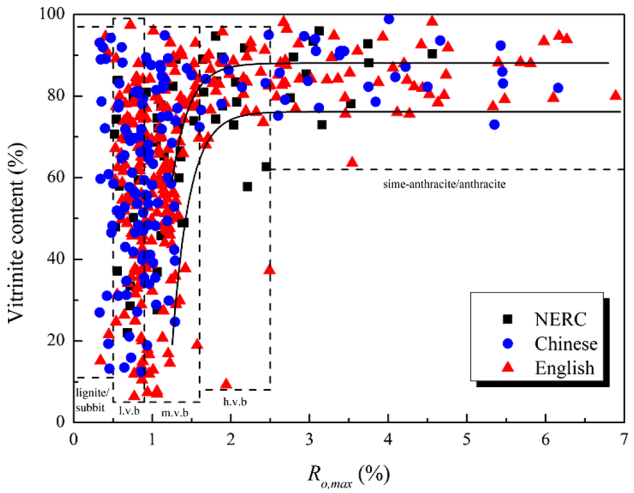

Fig. 9 Variation of vitrinite content with vitrinite reflectance $R_{o,max}$. (Data size: NERC-61, Chinese (Yu et al. 2004; Chang et al. 2006; Qin et al. 2007; Chang et al. 2008; Jiang et al. 2012; Lin et al. 2013; Xu and Pan 2015; Xiao et al. 2016)-159, English(Gan et al. 1972; Nelson et al. 1980; Giuliani et al. 1991; Crosdale et al. 1998; Marecka and Mianowski 1998; Bustin and Clarkson 1998; Laxminarayana and Crosdale 2002; Busch et al. 2003; Mastalerz et al. 2004; Hildenbrand et al. 2006; Busch et al. 2006; Siemons et al. 2007; Busch et al. 2007; Faiz et al. 2007a, b; Majewska and Ziętek 2007; Yu et al. 2008a, b, c; Astashov et al. 2008; Day et al. 2008; Mazumder and Wolf 2008; Pone et al. 2009; Majewska et al. 2009; Radliński et al. 2009; Battistutta et al. 2010; Gensterblum et al. 2010; He et al. 2010; Kim et al. 2011; Day et al. 2011; Le Gal et al. 2012; Maphala and Wagner 2012; Sakurovs 2012; An et al. 2013; Cai et al. 2013a, b; Dutka et al. 2013)-292)

$$Vitrinite = k_{\text{vitr}} c_{\text{vitr}}^{R_{\text{o,max}}} + b_{\text{vitr}} \tag{31}$$

where k_{vitr}, c_{vitr}, b_{vitr} are the coefficients in Eq. (31) and $k_{\text{vitr}} < 0$, $c_{\text{iner}} < 1$.

The first and order derivative are separately shown in Eqs. (32) and (33):

$$Vitrinite' = k_{\text{vitr}} \ln c_{\text{vitr}} c_{\text{vitr}}^{R_{\text{o,max}}} \tag{32}$$

$$Vitrinite'' = k_{\text{vitr}} \ln^2 c_{\text{vitr}} c_{\text{vitr}}^{R_{\text{o,max}}} \tag{33}$$

As $k_{\text{vitr}} < 0$, $c_{\text{iner}} < 1$, the first derivative (Eq. 32) of Eq. (31) is always greater than zero, while the second derivative (Eq. 33) is always less than zero, thus, it can be concluded that Eq. (31) exhibits up-convex, exponent-increasing type. It can be concluded that vitrinite content increases with the coal rank and at low metamorphic stage, vitrinite content increases greatly. The reason is: with the increase of metamorphism degree, exinite continuously generate hydrocarbon with a decreasing rate; in the stage of low metamorphic degree, exinite experience decarboxylation and the generation of oil process; the mid metamorphic stage experiences the transformation of gaseous hydrocarbons process. Therefore, in the stage of low metamorphic degree, is commonly seen, to mid metamorphic stage degree, the number of exinite reduced resulting in the increase of vitrinite content.

Besides, Fig. 9 shows that the minimum value of vitrinite content are generally larger than the curve expressed in the following equal: $Vitrinite_{\min} = 76.14 - 16996 \cdot 0.01063^{R_{\text{o,max}}}$, and the corresponding curve is $Vitrinite_{\text{avr}} = 88.07 - 8498 \times 0.01063^{R_{\text{o,max}}}$. The ranges of vitrinite content in subbituminous coal are from 11% to 97%, in low volatile bituminous coal are from 5% to 99%, in mid volatile bituminous coal are from 5% to 97%, in high volatile bituminous coal are from 8% to 97%, in anthracite are from 62% to 97%.

Combing Eqs. (31) and (12), the following Eq. (34) can be obtained:

$$Q = \frac{k_{\text{Q}}}{\ln c_{\text{vitr}}} \ln\left(\frac{Vitrinite - b_{\text{vitr}}}{k_{\text{vitr}}}\right) + b_{\text{Q}} \tag{34}$$

$$Q' = \frac{k_{\text{Q}}}{\ln c_{\text{vitr}}} \frac{1}{Vitrinite - b_{\text{vitr}}} \tag{35}$$

$$Q'' = \frac{-k_{\text{Q}}}{\ln c_{\text{vitr}}} \frac{1}{(Vitrinite - b_{\text{vitr}})^2} \tag{36}$$

As $k_{\text{Q}} > 0$, $c_{\text{vitr}} < 1$, $\ln c_{\text{iner}} < 0$, so $\frac{k_{\text{Q}}}{\ln c_{\text{iner}}} < 0$, and also because $k_{\text{vitr}} < 0$, the first derivative (Eq. 35) of Eq. (34) is always greater than zero, while the second derivative (Eq. 36) is always greater than zero, thus, it can be concluded that Eq. (34) exhibits depression, logarithmic-increasing type. It can be concluded that there is a positive relationship between gas content and vitrinite content and at low vitrinite content stage, gas content increases slowly. This is because of the loose structure of coal sample with the higher vitrinite content, the less water absorption, the formation of the gel like network structure. Besides, with the increase of metamorphism degree, there are more volatile matter produced in vitrinite, resulting in the increase in the number of micropores, the increase of the surface area and the adsorption capacity of coal.

4.2.2 Inertinite content effect on adsorption capacity

Inertinite is one of the common macerals in coal, and its content is lower than that of vitrinite in coal, It is made of wood carbonization products of fibrous tissue in the peat swamps, under oxidizing conditions, plant body experience a greater degree of aromatic condensation due to the loss of oxidized atoms resulting in the dehydrogenation and dehydration, The most common inertinite components are fusinite, fusovitrite and macrinite. According to the structure and morphology of cell, Inertinite is divided into fusinite, half fusinite, fungus, secretion, coarse grain, particles, debris of inertinite, etc. Figure 10 shows the

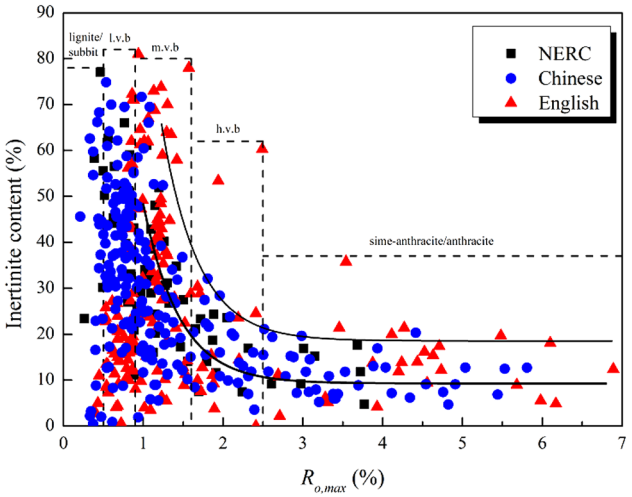

Fig. 10 Variation of Intertinite content with vitrinite reflectance $R_{o,max}$. (Data size: NERC-64, Chinese (Ceglarska-Stefańska and Brzóska 1998; Yu et al. 2004; Chang et al. 2006; Qin et al. 2007; Faiz et al. 2007a, b; Chang et al. 2008; Jiang et al. 2012; Lin et al. 2013; Xiao et al. 2016)-233, English(Giuliani et al. 1991; Crosdale et al. 1998; Bustin and Clarkson 1998; Marecka and Mianowski 1998; Laxminarayana and Crosdale 2002; Busch et al. 2003; Mastalerz et al. 2004; Busch et al. 2006; Hildenbrand et al. 2006; Busch et al. 2007; Majewska and Ziętek 2007; Siemons et al. 2007; Astashov et al. 2008; Day et al. 2008; Yu et al. 2008a, b; Mazumder and Wolf 2008; Pone et al. 2009; Radliński et al. 2009; Majewska et al. 2009; Gensterblum et al. 2010; Battistutta et al. 2010; He et al. 2010; Day et al. 2011; Kim et al. 2011; Maphala and Wagner 2012; Sakurovs 2012; An et al. 2013; Cai et al. 2013a, b; Dutka et al. 2013)-169)

relationship between inertinite and Vitrinite reflectance ($R_{o,max}$).

Figure 10 shows that the relationship between inertinite and vitrinite reflectance can be expressed in Eq. (37)

$$Inertinite = k_{iner} c_{iner}^{R_{o,max}} + b_{iner} \tag{37}$$

where k_{iner}, c_{iner}, b_{iner} are the coefficients in Eq. (37) and $k_{iner} > 0$, $c_{iner} < 1$.

The first and order derivative are separately shown in Eqs. (38) and (39):

$$Inertinite = k_{iner} \ln c_{iner} c_{iner}^{R_{o,max}} \tag{38}$$

$$Inertinite'' = k_{iner} \ln^2 c_{iner} c_{iner}^{R_{o,max}} \tag{39}$$

As $k_{iner} > 0$, $c_{iner} < 1$,the first derivative (Eq. 38) of Eq. (37) is always less than zero, while the second derivative (Eq. 39) is always greater than zero, thus, it can be concluded that Eq. (37) exhibits depression, exponent-decreasing type, that is the relationship between inertinite and vitrinite reflectance presents negative exponential correlation. Inertinite is negative exponential decline with the increase of metamorphism degree, and at the low metamorphism degree inertinite decreases largely.

Figure 10 shows that the data for the relationship between inertinite and vitrinite reflectance are more dispersed, and its maximum value did not exceed the upper curve with the following equation: $Inertinite_{max} = 18.557 + 706.1 \cdot 0.11058^{R_{o,max}}$, and the corresponding average curve is: $Inertinite_{avr} = 9.2785 + 353.05 \times 0.11058^{R_{o,max}}$. The ranges of inertinite content in subbituminous coal are from 0% to 78%, in low volatile bituminous coal are from 0% to 82%, in mid volatile bituminous coal are from 0 to 80 in high volatile bituminous coal are from 0% to 62%, in anthracite are from 0% to 37%.

Combing Eqs. (37) and (12), the Eq. (40) can be obtained:

$$Q = \frac{k_Q}{\ln c_{iner}} \ln\left(\frac{Inertinite - b_{iner}}{k_{iner}}\right) + b_Q \tag{40}$$

$$Q' = \frac{k_Q}{\ln c_{iner}} \frac{1}{Inertinite - b_{iner}} \tag{41}$$

$$Q'' = \frac{-k_Q}{\ln c_{iner}} \frac{1}{(Inertinite - b_{iner})^2} \tag{42}$$

As $k_Q > 0$, $c_{iner} < 1$, so $\ln c_{iner} < 0$, the first derivative (Eq. 41) of Eq. (40) is always less than zero, while the second derivative (Eq. 42) is always greater than zero, thus, it can be concluded that Eq. (40) exhibits depression logarithmic-decreasing type. That is, the gas content has a negative relationship with inertinite content, and at the low inertinite content stage, gas content decreases largely. The reason is that: inertinite has the greatest proportion of pores, a smaller surface area, and has a lot of internal oxygen functional groups and, therefore, has a weak adsorption capacity.

4.3 Ultimate analysis effect on adsorption capacity

Coal contains a lot of elements, but as the coal organic matter composition, the mainly five elements is carbon, hydrogen, oxygen, nitrogen, sulfur. These elements content are related to the formation of coal type, coal and rock composition and the degree of coalification. The different elements show not only the degree of coal metamorphism, but also reflect the coal nature. Carbon, hydrogen, and oxygen of Coal are mainly aromatic structure, aliphatic and alicyclic structure, the sum occupies more than 95%, and thus play major role in the adsorption ability of coal, and so, this paper mainly studies the three elements effect on the coal adsorption abilities.

4.3.1 Carbon content effect on adsorption capacity

Carbon is an important component of organic matter in coal. It is the main element of hex-acyclic-ring in the coal structure. A small amount of carbon is present in carbonate and carbon dioxide, and the content of carbon in coal is higher than that in any other element. Therefore, the

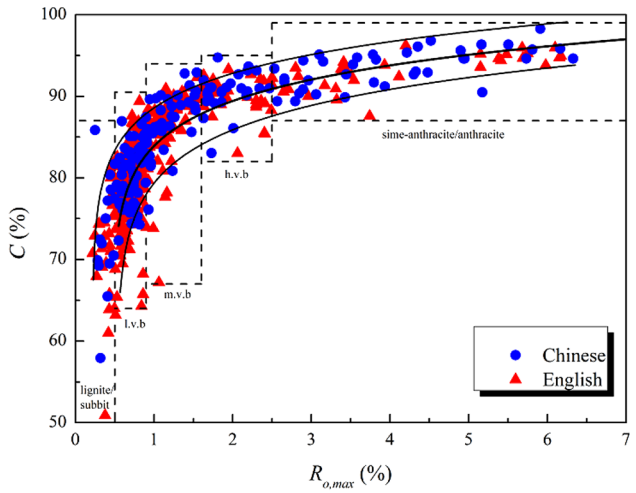

Fig. 11 Variation of C content with vitrinite reflectance $R_{o,max}$. (Data size: Chinese (Ceglarska-Stefańska and Brzóska 1998; Chang et al. 2006; Qin et al. 2007; Chang et al.; Lin et al. 2013)-169, English (Allardice and Evans 1971; Bhattacharyya 1972; Gan et al. 1972; Joubert et al. 1973, 1974; Nandi and Walker 1975; Nelson et al. 1980; Yang and Saunders 1985; Reucroft and Patel 1986; Banerjee 1988; Friesen and Mikula 1988; Giuliani et al. 1991; DeGance et al. 1993; Ciembroniewicz and Marecka 1993; Milewska-Duda et al. 1994; Chaback et al. 1996; Martyniuk and Więckowska 1997; Xu et al. 1997; Marecka and Mianowski 1998; Nodzeński 1998; Wang and Takarada 2003; Fitzgerald et al. 2005; Bae and Bhatia 2006; Dai et al. 2006; Siemons et al. 2007; Busch et al. 2007; Majewska and Ziętek 2007; Day et al. 2008; Majewska et al. 2009; Pone et al. 2009; Kędzior 2009; Radliński et al. 2009; Battistutta et al. 2010; Majewska et al. 2010; Gensterblum et al. 2010; He et al. 2010; Taraba 2011; Kim et al. 2011; Sakurovs 2012; Hao et al. 2013)-277)

metamorphism degree of coal is often referred to as carbonization degree. In order to reduce the impact of ash, moisture and other content, we use ash-free basis Dry indicator, Fig. 11 shows the relationship between carbon and vitrinite reflectance ($R_{o,max}$).

Figure 11 shows that the relationship between carbon content and vitrinite reflectance can be expressed in Eq. (23)

$$C_{daf} = k_C \ln(R_{o,max} + b_C) + d_C \tag{43}$$

where k_C, b_C, d_C are the coefficients in Eq. (43) and $k_C > 0$.

Solution of the first and the second derivative of Eq. (43) are shown in (44) and (45):

$$C'_{daf} = \frac{k_C}{R_{o,max} + b_C} \tag{44}$$

$$C''_{daf} = \frac{-k_C}{(R_{o,max} + b_C)^2} \tag{45}$$

As $k_C > 0$, the first derivative (Eq. 44) of Eq. (43) is always greater than zero, while the second derivative (Eq. 45) is always less than zero, thus, it can be concluded that Eq. (43) exhibits up-convex, logarithmic-increasing type. That is, the content of carbon in coal increases with the increase of metamorphism degree. In the stage of low metamorphic grade, the increase of carbon content is larger. The reason is that: with the increase of coal rank, the microstructure of coal tends to be regular. Figure 11 shows that the data for the relationship between carbon content and vitrinite reflectance are limited in the upper and downward curves: $C_{daf,max} = 89.83 + 5.16\ln(R_{o,max} - 0.215)$ and $C_{daf,min} = 83.62 + 5.788\ln(R_{o,max} - 0.522)$, The corresponding average curve is: $C_{daf,avr} = 87.21 + 5.216\ln(R_{o,max} - 0.47)$, The ranges of carbon content in subbituminous coal are from 0% to 87%, in low volatile bituminous coal are from 64% to 90.5%, in mid volatile bituminous coal are from 67% to 94%, in high volatile bituminous coal are from 82% to 95%, in anthracite are from 87% to 99%. The reason is that at the low metamorphism degree, due to the shallow bury, compaction and maturity is not high, so that the carbon content of coal is less.

Combing Eqs. (43) and (12), The Eq. (46) can be obtained:

$$Q = k_Q\left[exp\left(\frac{C_{daf} - d_C}{k_C}\right) - b_C\right] + b_Q \tag{46}$$

$$Q' = \frac{k_Q}{k_C} exp\left(\frac{C_{daf} - d_C}{k_C}\right) \tag{47}$$

$$Q'' = \frac{k_Q}{k_C^2} exp\left(\frac{C_{daf} - d_C}{k_C}\right) \tag{48}$$

As $k_Q > 0$, $k_C > 0$, the first and second derivatives (Eqs. 47 and 48) of Eq. (46) are always greater than zero, thus, it can be concluded that Eq. (46) exhibits depression, exponent - increasing type, That is, under the condition of the same temperature, adsorption capacity of coal increases with the increase of carbon content, and at the low carbon content stage, the gas content increases slowly. This is due to the increase of carbon content with the increase of coal rank, and the microstructure of coal tends to be regular. With the increase of $R_{o,max}$, the total porosity of coal increases, especially for small pores. The pore specific surface area of the coal is increasing, the adsorption capacity of coal is increasing, and the adsorption ability of methane is enhanced.

4.3.2 Hydrogen content effect on adsorption capacity

The importance of Hydrogen in coal is second only to the Carbon element, because of its minimum atomic mass, the number of atoms and Carbon elements are in the same magnitude order, and even more than Carbon elements. Hydrogen is also an important element in the composition of coal macromolecular backbone and side-chain,

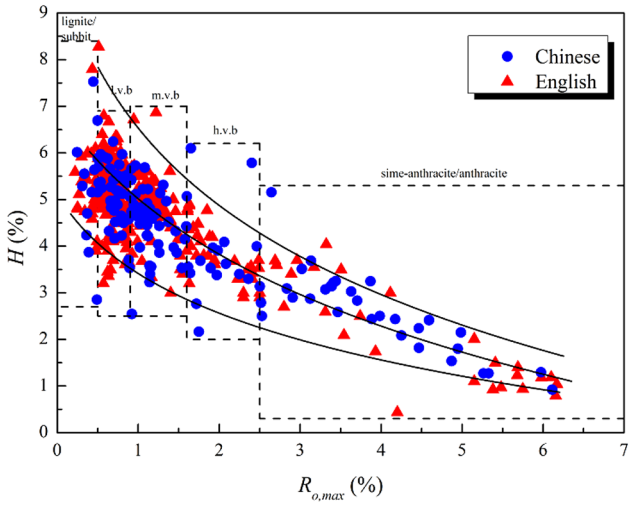

Fig. 12 Variation of H content with vitrinite reflectance $R_{o,max}$. (Data size: Chinese (Chang et al. 2006; Qin et al. 2007; Chang et al. 2008; Lin et al. 2013)-152, English(Allardice and Evans 1971; Bhattacharyya 1972; Gan et al. 1972; Joubert et al. 1973, 1974; Nandi and Walker 1975; Yang and Saunders 1985; Reucroft and Patel 1986; Banerjee 1988; Friesen and Mikula 1988; Giuliani et al. 1991; DeGance et al. 1993; Chaback et al. 1996; Marecka and Mianowski 1998; Martyniuk and Więckowska 1997; Wang and Takarada 2003; Fitzgerald et al. 2005; Dai et al. 2006; Bae and Bhatia 2006; Siemons et al. 2007; Majewska and Ziętek 2007; Day et al. 2008; Pone et al. 2009; Radliński et al. 2009; Majewska et al. 2009; Kędzior 2009; Majewska et al. 2010; Battistutta et al. 2010; Gensterblum et al. 2010; He, et al. 2010; Kim et al. 2011; Taraba 2011; Sakurovs 2012; Hao et al. 2013)-220)

compared with the carbon element, hydrogen has greater reaction capacity, hydrogen elements content is different in different types of coal. Figure 12 shows the relationship between Hydrogen content and vitrinite reflectance ($R_{o,max}$).

Hydrogen content are closely related to coal rank. Figure 12 shows that the relationship between Hydrogen content and vitrinite reflectance can be expressed by Eq. (49).

$$H_{daf} = k_H \ln(R_{o,max} + b_H) + d_H \tag{49}$$

where k_H, b_H, d_H are the coefficients in Eq. (49),and $k_H < 0$.

The solution of the first and second derivative of Eq. (49) are shown in Eqs. (50) and (51):

$$H'_{daf} = \frac{k_H}{R_{o,max} + b_H} \tag{50}$$

$$H''_{daf} = \frac{-k_H}{(R_{o,max} + b_H)^2} \tag{51}$$

As $k_H < 0$, the first derivative (Eq. 50) of Eq. (49) is always less than zero, while the second derivative (Eq. 51) is always greater than zero, thus, it can be concluded that Eq. (49) exhibits depression, logarithmic-decreasing type, That is the hydrogen content decreases with the increases of coal rank, and at the low coal rank, The hydrogen content decreases greatly.

Figure 12 shows that the data of the relationship between hydrogen content and coal rank has the limits of the upper and downward curves expressed in the following Equations: $H_{daf,max} = 7.87474 - 3.26191 \ln(R_{o,max} + 0.50856)$; $H_{daf,min} = 4.27974 - 1.77558 \ln(R_{o,max} + 0.62858)$, the equation for the corresponding average curve is: $H_{daf,avr} = 7.50833 - 3.16908 \ln(R_{o,max} + 1.19543)$, The ranges of hydrogen content in subbituminous coal are from 2.7% to 8.4%, in low volatile bituminous coal are from 2.5% to 6.9%, in mid volatile bituminous coal are from 2.5% to 7%, in high volatile bituminous coal are from 2% to 6.2%, in anthracite are from 0.3% to 5.3%. The reason for this change is the formation of low metamorphic coal from the Low hydrogen containing organisms.

Combing Eqs. (49) and (12), the Eq. (52) can be obtained:

$$Q = k_Q \left[exp\left(\frac{H_{daf} - d_H}{k_H} \right) - b_H \right] + b_Q \tag{52}$$

$$Q' = \frac{k_Q}{k_H} exp\left(\frac{H_{daf} - d_H}{k_H} \right) \tag{53}$$

$$Q'' = \frac{k_Q}{k_H^2} exp\left(\frac{H_{daf} - d_H}{k_H} \right) \tag{54}$$

As $k_Q > 0$, $k_H < 0$, the first derivative (Eq. 53) of Eq. (52) is always less than zero, while the second derivative (Eq. 54) is always greater than zero, thus, it can be concluded that Eq. (52) exhibits depression, exponent-decreasing type, thus, the gas content dropped exponentially with the Dry ash-free basis hydrogen content. The reason is that coal methyl and methylene chain increases the methane adsorption trap in coal, enhances adsorption ability of methane on coal surface. And with the increase in metamorphic grade, side chain of coal decreased, resulting in the hydrogen element content. Contribution of hydrogen to the overall coal adsorption capacity is negative.

4.3.3 Oxygen content effect on adsorption capacity

Oxygen is one of the main elements of coal and mainly consists of carboxyl (−COOH), hydroxyl (−OH−), carbonyl, methoxyl (−OCH_3−), and ether groups (–C–O–C–), and some of the oxygen combing with carbon skeleton into a heterocyclic ring (White 1909). The total amount and shape of oxygen in coal have a direct influence on the coal properties. Figure 13 shows the relationship between Oxygen content and vitrinite reflectance ($R_{o,max}$).

Figure 13 shows the relationship between oxygen content and vitrinite reflectance:

$$O_{daf} = k_O b_O^{R_{o,max}} + d_O \tag{55}$$

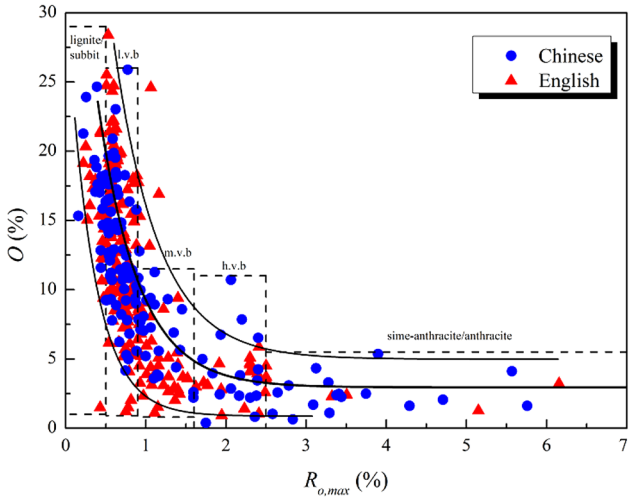

Fig. 13 Variation of O content with vitrinite reflectance $R_{o,max}$. (Data size:Chinese (Chang et al. 2006; Qin et al. 2007; Chang et al. 2008; Lin et al. 2013)-145, English(Allardice and Evans 1971; Gan et al. 1972; Joubert et al. 1973, 1974; Nandi and Walker 1975; Nelson et al. 1980; Yang and Saunders 1985; Reucroft and Patel 1986; Banerjee 1988; Friesen and Mikula 1988; DeGance et al. 1993; Chaback et al. 1996; Wang and Takarada 2003; Fitzgerald et al. 2005; Dai et al. 2006; Bae and Bhatia 2006; Siemons et al. 2007; Majewska et al. 2009; Pone et al. 2009; Radliński et al. 2009; Battistutta et al. 2010; Gensterblum et al. 2010; He et al. 2010; Kim et al. 2011; Hao et al. 2013)-254)

where k_O, b_O, d_O are the coefficients in Eq. (55), and $k_O > 0$, $b_O < 1$.

The solutions of the first and second derivative for the Eq. (55) are shown in Eqs. (56) and (57):

$$Q'_{daf} = k_O \ln b_O b_O^{R_{o,max}} \tag{56}$$

$$O''_{daf} = k_O \ln^2 b_O b_O^{R_{o,max}} \tag{57}$$

As $k_O > 0$, the first derivative (Eq. 56) of Eq. (55) is always less than zero, while the second derivative (Eq. 57) is always greater than zero, thus, it can be concluded that Eq. (55) exhibits depression, exponent-decreasing type, that is,the oxygen content decreases with the increase of coal rank,and at the low metamorphic degree, the oxygen declines greatly. Reasons for this change is increases of oxygen content decreases the caking property of coal and increased the hydrogen bound, so side chain of the six carbon ring in young coal is more, and most of side chain polar groups are oxygen containing functional groups. Side chain will decrease with the coal rank, and finally resulting in the decrease of oxygen content.

Figure 13 shows that the data for the relationship between oxygen content and vitrinite reflectance exists upper and downward limits expressed in the equations: $O_{daf,max} = 4.98 + 67.19 \cdot 0.1655^{R_{o,max}}$, $O_{daf,min} = 0.866 + 30.482 \cdot 0.047^{R_{o,max}}$, the corresponding average curve is expressed in the following equation: $O_{daf,avr} = 2.943 + 45.555 \cdot 0.138^{R_{o,max}}$, from the dashed line in Fig. 13, it can be seen that: The ranges of oxygen content in subbituminous coal are from 1% to 29%, in low volatile bituminous coal are from 0.9% to 26%, in mid volatile bituminous coal are from 0.8% to 11.5%, in high volatile bituminous coal are from 0% to 11%, in anthracite are from 0% to 5.5%.

Combing the Eqs. (55) and (12), the Eq. (58) can be obtained:

$$Q = \frac{k_Q}{\ln b_O}[\ln(O_{daf} - d_O) - \ln k_O] + b_Q \tag{58}$$

$$Q' = \frac{k_Q}{\ln b_O}\frac{1}{O_{daf} - d_O} \tag{59}$$

$$Q'' = \frac{-k_Q}{\ln b_O}\frac{1}{(O_{daf} - d_O)^2} \tag{60}$$

As $k_Q > 0$, $b_O < 1$, $\ln b_O < 0$, so $\frac{k_Q}{\ln b_O} < 0$, the first derivative (Eq. 59) of Eq. (58) is always less than zero, while the second derivative (Eq. 60) is always greater than zero, thus, it can be concluded that Eq. (58) exhibits depression, logarithmic-decreasing type, that is the oxygen has a negative effect on gas adsorption capacity, and at the low oxygen content stage, the gas content decreases greatly. The reason is that the oxygen element exists in the form of oxygen functional groups in coal, And the oxygen functional groups of carboxyl, hydroxyl and aldehyde reduced the adsorption wells of methane, weakened the adsorption capacity of methane. Therefore, the reduction of oxygen functional groups in coal increases the adsorption capacity of coal. It was observed that there was, in general, a positive correlation between the methane saturated adsorption capacity and the micropore volume of coals while a negative correlation between methane saturated adsorption capacity and the O_{total}/C_{total}. Coal with a higher amount of oxygen surface groups, and consequently with a less hydrophobic character, had lower methane adsorption capacity.

4.4 Comprehensive analysis of physicochemical properties of coal effect on methane adsorption

The reason for the fixed carbon content increases with the coal rank is: In the process of coal metamorphism, the carbonization trend is obviously shown, that is, the low rank contains five kinds of elements of C, H, O, N, S, While, the anthracite basically only contain one element of carbon. The reason is that: the chemical components and the structure of coal changes in the process of coal metamorphic, the performance for this is the rot colonization material constantly aggregate, hydrophilic oxygen group such as hydroxyl and carboxyl lost large of water, from low

metamorphic degree of coal with variety functional groups structure, to anthracite containing condensation aromatic nuclear of structure, hydrophilic functional groups constantly reduced, carbon content constantly increases, resulting in the weaken of hydrophilic constantly and the adsorption of methane constantly enhanced. At the low metamorphic degree stage, the oxygen and hydrogen content in vitrinite are all greater than in inertinite,which means that the oxygen-containing groups of hydroxyl and carboxyl in vitrinite at this stage is higher, resulting in the higher hydrophilia and weakened gas adsorption capacity. Thus, at low metamorphic degree stage, the gas adsorption capacity of vitrinite is weaker than that of inertinite vitrinite, the reason is that with the increase of coal rank, hydrophilic group in vitrinite fall off, and the gas adsorption capacity can be strengthen.

5 Conclusions

Physicochemical properties of coal and the methane adsorption capacity had a well-regulated change with coal rank. Limit adsorption capacity expressed in a_{daf} decreases firstly and then increases with the increase of coal rank, but Adsorption constant of b falling in the range of 0.15–2.25 MP^{-1} present the opposite changing law. Dry ash-free basis gas content of Q_{daf} increases with increasing metamorphism of coal, and the gas content of raw coal (Q)increases linearity with the coal rank.

Fixed carbon, vitrinite, carbon element present the positive interrelated relationship to maximum vitrinite reflectance $R_{\mathrm{o,max}}$, and $R_{\mathrm{o,max}} \sim Fc_{\mathrm{ad}}$, $R_{\mathrm{o,max}} \sim Vitrinite$ exhibits power-decreasing type, $R_{\mathrm{o,max}} \sim C_{\mathrm{daf}}$ exhibits Logarithm function type. The volatile, inherent moisture, inertinite, oxygen content, hydrogen content present the negative interrelated relationship to maximum vitrinite reflectance $R_{\mathrm{o,max}}$,and $R_{\mathrm{o,max}} \sim V_{daf}$ exhibits power-decreasing type, $R_{\mathrm{o,max}} \sim M_{\mathrm{ad}}$, $R_{\mathrm{o,max}} \sim Inertinite$, $R_{\mathrm{o,max}} \sim O_{daf}$ exhibit exponential function type, and $R_{\mathrm{o,max}} \sim H_{daf}$ exhibit Logarithm function type. Furthermore, we can derive fixed carbon and vitrinite present a positive correlation with adsorption capacity of Q, and $Fc_{ad} \sim Q$ and $Vitrinite \sim Q$ are Logarithm function, while $C_{\mathrm{daf}} \sim Q$ exhibits exponential function type. Besides, volatile,vinherent moisture, inertinite, oxygen content, hydrogen content of coal present a negative correlation with adsorption capacity of Q, and $V_{\mathrm{daf}} \sim Q$ exhibits a power function type; $M_{\mathrm{ad}} \sim Q$, $Inertinite \sim Q$ and $O_{\mathrm{daf}} \sim Q$ exhibit Logarithm function type, while $H_{\mathrm{daf}} \sim Q$ is an exponential function.

The essence of the effect of coal rank on methane adsorption capacity is the changing of Physicochemical Properties of Coal.

Acknowledgements The authors are grateful to the National Science Foundation of China (No. 51379619), the National Science Foundation for the Youth of China (No. 51604187) and the Provincial Science Foundation for Young Scholars (Shanxi Province, China) (No. 201601D021091).

References

Allardice DJ, Evans DG (1971) The-brown coal/water system: Part 2. Water sorption isotherms on bed-moist Yallourn brown coal. Fuel 50:236–253

An FH, Cheng YP, Wu DM, Wang L (2013) The effect of small micropores on methane adsorption of coals from Northern China. Adsorpt J Int Adsorpt Soc 19:83–90

Astashov AV, Belyi AA, Bunin AV (2008) Quasi-equilibrium swelling and structural parameters of coals. Fuel 87:3455–3461

Bae J, Bhatia SK (2006) High-pressure adsorption of methane and carbon dioxide on coal. Energy Fuels 20:2599–2607

Banerjee BD (1988) Spacing of fissuring network and rate of desorption of methane from coals. Fuel 67:1584–1586

Barker-Read GR, Radchenko SA (1989) Methane emission from coal and associated strata samples. Int J Min Geol Eng 7:101–126

Battistutta E, Hemert PV, Lutynski M, Bruining H, Wolf K (2010) Swelling and sorption experiments on methane, nitrogen and carbon dioxide on dry Selar Cornish coal. Int J Coal Geol 84:39–48

Beamish BB, O'Donnell G (1992) Microbalance applications to sorption testing of coal. In: Coalbed Methane Symposium, pp 31–41, Townsville 19–21 November

Bhattacharyya KK (1972) The role of desorption of moisture from coal in its spontaneous heating. Fuel 51:214–220

Busch A, Gensterblum Y, Krooss BM (2003) Methane and CO_2 sorption and desorption measurements on dry Argonne premium coals: pure components and mixtures. Int J Coal Geol 55:205–224

Busch A, Gensterblum Y, Krooss BM, Siemons N (2006) Investigation of high-pressure selective adsorption/desorption behaviour of CO_2 and CH_4 on coals: an experimental study. Int J Coal Geol 66:53–68

Busch A, Gensterblum Y, Krooss BM (2007) High-pressure sorption of nitrogen, carbon dioxide, and their mixtures on argonne premium coals. Energy Fuels 21:1640–1645

Bustin RM, Clarkson CR (1998) Geological controls on coalbed methane reservoir capacity and gas content. Int J Coal Geol 38:3–26

Cai Y, Liu D, Pan Z, Yao Y, Li J, Qiu Y (2013a) Petrophysical characterization of Chinese coal cores with heat treatment by nuclear magnetic resonance. Fuel 108:292–302

Cai Y, Liu D, Pan Z, Yao Y, Li J, Qiu Y (2013b) Pore structure and its impact on CH_4 adsorption capacity and flow capability of

bituminous and subbituminous coals from Northeast China. Fuel 103:258–268
Ceglarska-Stefańska G, Brzóska K (1998) The effect of coal metamorphism on methane desorption. Fuel 77:645–648
Chaback JJ, Morgan WD, Yee D (1996) Sorption of nitrogen, methane, carbon dioxide and their mixtures on bituminous coals at in situ conditions. Fluid Ph Equilib 117:289–296
Chalmers GRL, Marc Bustin R (2007) On the effects of petrographic composition on coalbed methane sorption. Int J Coal Geol 69:288–304
Chang HZ, Wang CG, Zeng FG, Li J, Li WY, Xie KC (2006) XPS comparative analysis of coal macerals with different reducibility. J Fuel Chem Technol 34:389–394
Chang HZ, Cai XM, Li GX, Bai G, Lv XQ (2008) Characterization for the stacking structure of coal macerals with different type reductivity. J Shanxi Univ (Natural Science Edition) 31:223–227
Charrière D, Pokryszka Z, Behra P (2010) Effect of pressure and temperature on diffusion of CO_2 and CH_4 into coal from the Lorraine basin (France). Int J Coal Geol 81:373–380
Chen ZH, Wang YB, Song Y, Liu HL (2008) Comparison of adsorption/desorption properties of CBM in different-rank coals. Nat Gas Ind 28:30–32
Chen Y, Chen DL, Luo HZ (2010) Effect of moisture on methane adsorption of coal. Saf Coal Min 117–119
Chen S, Jin L, Chen X (2011) The effect and prediction of temperature on adsorption capability of coal/CH_4. Proced Eng 26:126–131
Ciembroniewicz A, Marecka A (1993) Kinetics of CO_2 sorption for two Polish hard coals. Fuel 72:405–408
Clarkson CR, Bustin RM (1999) The effect of pore structure and gas pressure upon the transport properties of coal: a laboratory and modeling study. 2. Adsorpt rate modeling. Fuel 78:1345–1362
Clarkson CR, Bustin RM (2000) Binary gas adsorption/desorption isotherms: effect of moisture and coal composition upon carbon dioxide selectivity over methane. Int J Coal Geol 42:241–271
Clarkson CR, Bustin RM, Levy JH (1997) Application of the mono/multilayer and adsorption potential theories to coal methane adsorption isotherms at elevated temperature and pressure. Carbon 35:1689–1705
Crosdale PJ, Beamish BB, Valix M (1998) Coalbed methane sorption related to coal composition. Int J Coal Geol 35:147–158
Crosdale PJ, Moore TA, Mares TE (2008) Influence of moisture content and temperature on methane adsorption isotherm analysis for coals from a low-rank, biogenically-sourced gas reservoir. Int J Coal Geol 76:166–174
Dai S, Han D, Chou C (2006) Petrography and geochemistry of the Middle Devonian coal from Luquan, Yunnan Province, China. Fuel 85:456–464
Day S, Duffy G, Sakurovs R, Weir S (2008) Effect of coal properties on CO_2 sorption capacity under supercritical conditions. Int J Greenh Gas Control 2:342–352
Day S, Fry R, Sakurovs R (2011) Swelling of moist coal in carbon dioxide and methane. Int J Coal Geol 86:197–203
DeGance AE, Morgan WD, Yee D (1993) High pressure adsorption of methane, nitrogen and carbon dioxide on coal substrates. Fluid Ph Equilib 82:215–224
Dutka B, Kudasik M, Pokryszka Z, Skoczylas N, Topolnicki J, Wierzbicki M (2013) Balance of CO_2/CH_4 exchange sorption in a coal briquette. Fuel Process Technol 106:95–101
Dutta P, Harpalani S, Prusty B (2008) Modeling of CO_2 sorption on coal. Fuel 87:2023–2036
Faiz MI, Aziz NI, Hutton AC, Jones B (1992) Porosity and gas sorption capacity of some eastern Australian coals in relation to coal rank and composition. In: Coalbed Methane Symposium, pp. 9–20, Townsville 19–21 November
Faiz M, Saghafi A, Sherwood N, Wang I (2007a) The influence of petrological properties and burial history on coal seam methane reservoir characterisation, Sydney Basin, Australia. Int J Coal Geol 70:193–208
Faiz MM, Saghafi A, Barclay SA, Stalker L, Sherwood NR, Whitford DJ (2007b) Evaluating geological sequestration of CO_2 in bituminous coals: the southern Sydney Basin, Australia as a natural analogue. Int J Greenh Gas Control 1:223–235
Fitzgerald JE, Pan Z, Sudibandriyo M, Robinson JRL, Gasem KAM, Reeves S (2005) Adsorption of methane, nitrogen, carbon dioxide and their mixtures on wet Tiffany coal. Fuel 84:2351–2363
Friesen WI, Mikula RJ (1988) Mercury porosimetry of coals: pore volume distribution and compressibility. Fuel 67:1516–1520
Fu XH, Qin Y, Li GZ, Xu L, Hu C (2002) Adsorption experiment of extra-high rank coal under the condition of equilibrium moisture content. Petroleum Geol Exp 24:177–180
Fu XH, Jiao ZF, Qin Y, Zhang WH, Han XX (2005) Adsorption experiments of low rank coal under equilibrium moistures. Journal of Liaoning Technical University 24:161–164
Fu XH, Qin Y, Quan B, Fan BH, Wang KX (2008) Study of physical and numerical simulations of adsorption methane content on middle-rank coal. Acta Geol Sin 82:1368–1371
Gan H, Nandi SP, Walker PL Jr (1972) Nature of the porosity in American coals. Fuel 51:272–277
Gao RC (2012) The adsorption/desorption of methane on tectonic coal based on adsorption potential theory. Henan Polytechnic University, 34–46
Gensterblum Y, Hemert PV, Billemont P, Battistutta E, Busch A, Krooss BM, Weireld GD, Wolf KHAA (2010) European inter-laboratory comparison of high pressure CO_2 sorption isotherms II: natural coals. Int J Coal Geol 84:115–124
Giuliani JD, Peirong W, Dyrkacz GR, Johns RB (1991) The characterization of two Australian bituminous coals and isolated maceral fractions by sequential pyrolysis-gas chromatography/mass spectrometry. J Anal Appl Pyrolysis 20:151–159
Hao SX, Wang CY, Jiang CF (2012) Influence of fixed carbon on coal textural character and methane adsorption capacity. J China Coal Soc 37(9):1477–1482
Hao S, Wen J, Yu X, Chu W (2013) Effect of the surface oxygen groups on methane adsorption on coals. Appl Surf Sci 264:433–442
He MC, Wang CG, Feng JL, Li DJ, Zhang GY (2010) Experimental investigations on gas desorption and transport in stressed coal under isothermal conditions. Int J Coal Geol 83:377–386
Hildenbrand A, Krooss BM, Busch A, Gaschnitz R (2006) Evolution of methane sorption capacity of coal seams as a function of burial history—a case study from the Campine Basin, NE Belgium. Int J Coal Geol 66:179–203
Jiang WP (2009) Microscopic mechanism study on the influence of coal rank on adsorption capacity. China Coalbed Methane, pp 19–22
Jiang JY, Cheng YP, Liang W, Guo PK, Feng-Hua AN (2012) The controlling effect of extremely thick igneous intrusions on coal and gas outburst. J China Univ Min Technol 41:42–47
Jin H, Schimmelmann A, Mastalerz M, Pope J, Moore TA (2010) Coalbed gas desorption in canisters: consumption of trapped atmospheric oxygen and implications for measured gas quality. Int J Coal Geol 81:64–72
Joubert JI, Grein CT, Bienstock D (1973) Sorption of methane in moist coal. Fuel 52:181–185
Joubert JI, Grein CT, Bienstock D (1974) Effect of moisture on the methane capacity of American coals. Fuel 53:186–191
Kędzior S (2009) Accumulation of coal-bed methane in the south-west part of the Upper Silesian Coal Basin (southern Poland). Int J Coal Geol 80:20–34

Kim HJ, Shi Y, He J, Lee H, Lee C (2011) Adsorption characteristics of CO_2 and CH_4 on dry and wet coal from subcritical to supercritical conditions. Chem Eng J 171:45–53

Kutchko BG, Goodman AL, Rosenbaum E, Natesakhawat S, Wagner K (2013) Characterization of coal before and after supercritical CO_2 exposure via feature relocation using field-emission scanning electron microscopy. Fuel 107:777–786

Laxminarayana C, Crosdale PJ (1999) Role of coal type and rank on methane sorption characteristics of Bowen Basin, Australia coals. Int J Coal Geol 40:309–325

Laxminarayana C, Crosdale PJ (2002) Controls on methane sorption capacity of Indian coals. AAPG Bull 86:201–212

Le Gal N, Lagneau V, Charmoille A (2012) Experimental characterization of CH_4 release from coal at high hydrostatic pressure. Int J Coal Geol 96–97:82–92

Levy JH, Day SJ, Killingley JS (1997) Methane capacities of Bowen Basin coals related to coal properties. Fuel 76:813–819

Li YB, Zhang YG, Zhang ZM, Jiang B (2013) Experimental study on gas desorption of tectonic coal at initial stage. J China Coal Soc 38:15–20

Lin HL, Li KJ, Zhang XW, Li YL (2013) Structural characterization of Shendong Shangwan coal and its maceral. Coal Convers 36:1–5

Liu ZN, Zhang H, Wang GR, Cheng AH, Wang Y (2015) Preparation and performance of coal based chelating adsorbent. J China Coal Soc 40:172–178

Ma JC, Wang B, Liu F, Liu HL, Li GZ, Zeng LJ (2008) Adsorption property of high-rank coal. Natural Gas Technology, pp 31–34

Ma XZ, Song Y, Liu SB, Jiang L, Hong F (2014) Quantitative research on adsorption capacity evolution of middle-high rank coal reservoirs in geological history: a case study from Hancheng Area in Ordos Basin. Acta Petrolei Sin 35:1080–1086

Mahajan OP, Walker PL Jr (1971) Water adsorption on coals. Fuel 50:308–317

Majewska Z, Ziętek J (2007) Changes of acoustic emission and strain in hard coal during gas sorption–desorption cycles. Int J Coal Geol 70:305–312

Majewska Z, Ceglarska-Stefańska G, Majewski S, Ziętek J (2009) Binary gas sorption/desorption experiments on a bituminous coal: simultaneous measurements on sorption kinetics, volumetric strain and acoustic emission. Int J Coal Geol 77:90–102

Majewska Z, Majewski S, Ziętek J (2010) Swelling of coal induced by cyclic sorption/desorption of gas: experimental observations indicating changes in coal structure due to sorption of CO_2 and CH_4. Int J Coal Geol 83:475–483

Maphala T, Wagner NJ (2012) Effects of CO_2 storage in coal on coal properties. Energy Proced 23:426–438

Marecka A, Mianowski A (1998) Kinetics of CO_2 and CH_4 sorption on high rank coal at ambient temperatures. Fuel 77:1691–1696

Mares TE, Moore TA (2008) The influence of macroscopic texture on biogenically-derived coalbed methane, Huntly coalfield, New Zealand. Int J Coal Geol 76:175–185

Martyniuk H, Więckowska J (1997) The effect of coal rank and carbonization temperature on SO_2 adsorption properties of coal chars. Fuel 76:563–565

Mastalerz M, Gluskoter H, Rupp J (2004) Carbon dioxide and methane sorption in high volatile bituminous coals from Indiana, USA. Int J Coal Geol 60:43–55

Mastalerz M, Solano-Acosta W, Schimmelmann A, Drobniak A (2009) Effects of coal storage in air on physical and chemical properties of coal and on gas adsorption. Int J Coal Geol 79:167–174

Mazumder S, Wolf KH (2008) Differential swelling and permeability change of coal in response to CO_2 injection for ECBM. Int J Coal Geol 74:123–138

Milewska-Duda J, Ceglarska-Stefańska G, Duda J (1994) A comparison of theoretical and empirical expansion of coals in the high pressure sorption of methane. Fuel 73:975–979

Nandi SP, Walker PL Jr (1975) Activated diffusion of methane from coals at elevated pressures. Fuel 54:81–86

Nelson JR, Mahajan OP, Walker PL Jr (1980) Measurement of swelling of coals in organic liquids: a new approach. Fuel 59:831–837

Nodzeński A (1998) Sorption and desorption of gases (CH_4, CO_2) on hard coal and active carbon at elevated pressures. Fuel 77:1243–1246

Özgen Karacan C, Okandan E (2000) Assessment of energetic heterogeneity of coals for gas adsorption and its effect on mixture predictions for coalbed methane studies. Fuel 79:1963–1974

Pan JN, Xu HF (2015) Study on characteristics of adsorption/desorption of medium and high rank tectonic deformation coals in Henan province. Coal Science and Technology, pp 29–32

Pan Z, Connell LD, Camilleri M, Connelly L (2010) Effects of matrix moisture on gas diffusion and flow in coal. Fuel 89:3207–3217

Pini R, Ottiger S, Storti G, Mazzotti M (2009) Pure and competitive adsorption of CO_2, CH_4 and N_2 on coal for ECBM. Energy Proced 1:1705–1710

Pini R, Marx D, Burlini L, Storti G, Mazzotti M (2011) Coal characterization for ECBM recovery: gas sorption under dry and humid conditions, and its effect on displacement dynamics. Energy Proced 4:2157–2161

Pone JDN, Halleck PM, Mathews JP (2009) Sorption capacity and sorption kinetic measurements of CO_2 and CH_4 in confined and unconfined bituminous coal. Energy Fuels 23:4688–4695

Qin ZH, Hou CL, Di Z, Ding SG, Hao S, Jiang C (2007) Characteristics of micropore-inbuilt form of micromolecules in coal and their solubilization rules. J China Univ Min Technol 36:586–591

Radliński AP, Busbridge TL, Gray EMA, Blach TP, Cookson DJ (2009) Small angle X-ray scattering mapping and kinetics study of sub-critical CO_2 sorption by two Australian coals. Int J Coal Geol 77:80–89

Reich MH, Snook IK, Wagenfeld HK (1992) A fractal interpretation of the effect of drying on the pore structure of Victorian brown coal. Fuel 71:669–672

Ren ZY (2010) The studies on adsorption of methane, carbon dioxide gas on the anthracite coal of Yang Quan. Henan Polytechnic University. p 81

Reucroft PJ, Patel H (1986) Gas-induced swelling in coal. Fuel 65:816–820

Saghafi A, Faiz M, Roberts D (2007) CO_2 storage and gas diffusivity properties of coals from Sydney Basin, Australia. Int J Coal Geol 70:240–254

Sakurovs R (2012) Relationships between CO_2 sorption capacity by coals as measured at low and high pressure and their swelling. Int J Coal Geol 90–91:156–161

Siemons N, Wolf KAA, Bruining J (2007) Interpretation of carbon dioxide diffusion behavior in coals. Int J Coal Geol 72:315–324

Su XB, Zhang LP, Lin XY (2005) Influence of coal rank on coal adsorption capacity. Nat Gas Ind 25:19–21

Su XB, Liu GW, Guo SQ, Lin XY (2006) Relationship of coalbed methane adsorption potential and coal rank. China Coalbed Methane, Beijing, pp 21–23

Taraba B (2011) Flow calorimetric insight to competitive sorption of carbon dioxide and methane on coal. Thermochim Acta 523:250–252

Tian L, Zheng BP, Yuan TX (2010) Adsorption characteristics and influence factors of high -rank coal bed methane in the Gaojiazhuang Area of Qinshui Basin. Journal of Hebei University of Engineering (Natural Science Edition), 57–61

Unsworth JF, Fowler CS, Jones LF (1989) Moisture in coal: 2 Maceral effects on pore structure. Fuel 68:18–26

Wang FQ (2012) The research on law of gas deposition in A Dao hai Mining, pp. 17–24. Inner Mongolia University of Science and Technology, Baotou

Wang J, Takarada T (2003) Characterization of high-temperature coal tar and supercritical-water extracts of coal by laser desorption ionization-mass spectrometry. Fuel Process Technol 81:247–258

Wang KX, Fu XH, Quan B, Wang JR, Shen J (2008) Study on the adsorption/desorption characteristics of various rank coals in China: 2008 CBM Symposium, p 12, China Jing gang shan in Jiangxi Province

Weishauptová Z, Medek J, Kovář L (2004) Bond forms of methane in porous system of coal II. Fuel 83:1759–1764

White D (1909) The effect of oxygen in coal. Department of the Interior United States Geological Survey, George Otjs Smith, Director, Bulletin 382

Xiao ZG, Wang ZF (2011) Experimental study on inhibitory effect of gas desorption by injecting water into coal-sample. Proced Eng 26:1287–1295

Xiao CY, Wei CT, Guo LW (2016) Carbon monoxide adsorption and desorption features of medium and low rank coal. Coal Science and Technology, pp 98–102

Xu HF, Pan JN (2015) Nanoscale pore structures of medium and high rank tectonic deformed coal and their influence on methane adsorption. Safety in Coal Mines, pp 27–30

Xu L, Zhang D, Xian X (1997) Fractal dimensions of coals and cokes. J Colloid Interface Sci 190:357–359

Yalçin E, Durucan Ş (1991) Methane capacities of Zonguldak coals and the factors affecting methane adsorption. Min Sci Technol 13:215–222

Yang RT, Saunders JT (1985) Adsorption of gases on coals and heat treated coals at elevated temperature and pressure: 1. Adsorption from hydrogen and methane as single gases. Fuel 64:616–620

Yang ZY, Zhang H, Zhang Q, Li HT, Li JW (2009) Mechanism of uranyl ion adsorbing and complexing onto low-rank coal and ore-forming process of uranium associated coal measures. Coal Geol Explor 37:1–5

Yao Y, Liu D (2012) Effects of igneous intrusions on coal petrology, pore-fracture and coalbed methane characteristics in Hongyang, Handan and Huaibei coalfields, North China. Int J Coal Geol 96–97:72–81

Yao Y, Liu D, Huang W (2011) Influences of igneous intrusions on coal rank, coal quality and adsorption capacity in Hongyang, Handan and Huaibei coalfields, North China. Int J Coal Geol 88:135–146

Yu HG, Fan WT, Sun MY, Ye JP (2004) Study on fitting models for methane isotherms adsorption of coals. J China Coal Soc 29:463–467

Yu HG, Fan WT, Sun MY, Ye JP (2005) Characteristics and predictions for adsorption isotherms of methane/carbon dioxide binary gas on coals. J China Coal Soc 30:76–80

Yu YJ, Wang YH, Yang Q, Liu DM, Hu BL, Huang WH, Che Y (2008a) Adsorption characteristics of low-rank coal reservoirs and coalbed methane development potential, Junggar Basin. Petroleum Explor Dev 35:410–416

Yu H, Yuan J, Guo W, Cheng J, Hu Q (2008b) A preliminary laboratory experiment on coalbed methane displacement with carbon dioxide injection. Int J Coal Geol 73:156–166

Yu H, Zhou L, Guo W, Cheng J, Hu Q (2008c) Predictions of the adsorption equilibrium of methane/carbon dioxide binary gas on coals using Langmuir and ideal adsorbed solution theory under feed gas conditions. Int J Coal Geol 73:115–129

Yue JW, Yue GW, Cao HS (2016) Mechanism analysis on adsorption properties of soft and hard coal based on adsorption layer thickness theory. Journal of China Coal Society, 653–661

Zhang QL (2007) Research on binary gas sorption on coal with different coal ranks. Petroleum Geol Exp 29:436–440

Zhang QL (2008) Adsorption mechanism of different coal ranks under variable temperature and pressure conditions. J China Univ Min Technol 18:395–400

Zhang SY, Sang SX (2008) Influence mechanism of liquid water on methane absorption of coals with different ranks. Acta Geol Sin 82:1350–1354

Zhang SY, Sang SX (2009) Adsorption-diffusion coefficient analysis of coal-bed methane in different rank coals. Coal Geol China 21:24–27

Zhang Q, Yang XL (1999) Isothermal adsorption of coals on methane under equilibrium moisture. J China Coal Soc 24:566–570

Zhang QL, Cui YJ, Cao LG (2004) Influence of pressure on adsorption ability of coal with different deterioration level. Nat Gas Ind 24:98–100

Zhang DF, Cui YJ, Li SG, Song WL, Lin WG (2011) Adsorption and diffusion behaviors of methane and carbon dioxide on various rank coals. J China Coal Soc 36:1693–1698

Zhang WJ, Ju YW, Kong XW, Hou QL, Wei MM, Li XS, Yu LY (2014) Structure and composition characteristics of deformed high-rank coals in the south of Qinshui basin and their influence on CBM adsorption/desorption. J Univ Chinese Acad Sci 31:98–107

Zheng GQ (2012) Experimental and simulation study on the sorption, diffusion and seepage characters in different-ranked coals. China University of Geosciences (Beijing), pp 26–46

Zou WJ, Cao YJ, Li WN, Liu JT, Wang YT (2013) Selective flocculation of coal and kaolinite. J China Coal Soc 38:1448–1453